CHAPTER-5

Results and Discussion

5.1Preformulation studies

5.1.1Physical appearance

Gift sample of CAP provided by Cipla Ltd. Bangalore, India was obtained in a press sealed polyethylene pack. The samplewas identified and characterizedby observing its morphological property.The sample of CAP appeared as a white crystalline powder with a mild bitter taste.

5.1.2 Melting point

The melting point of the drug sample was found to be 121°C that was found to be similar as reported officially.

5.1.3 FTIR

The FTIR spectrum of the drug showed several distinctive peaks complying with reference peaks of CAP mentioned in the literature. This confirms that the obtained sample of CAP was a pure drug. The image of the absorption spectrum and the bands are mentioned in Figure 5.1 and Table 5.1 respectively.

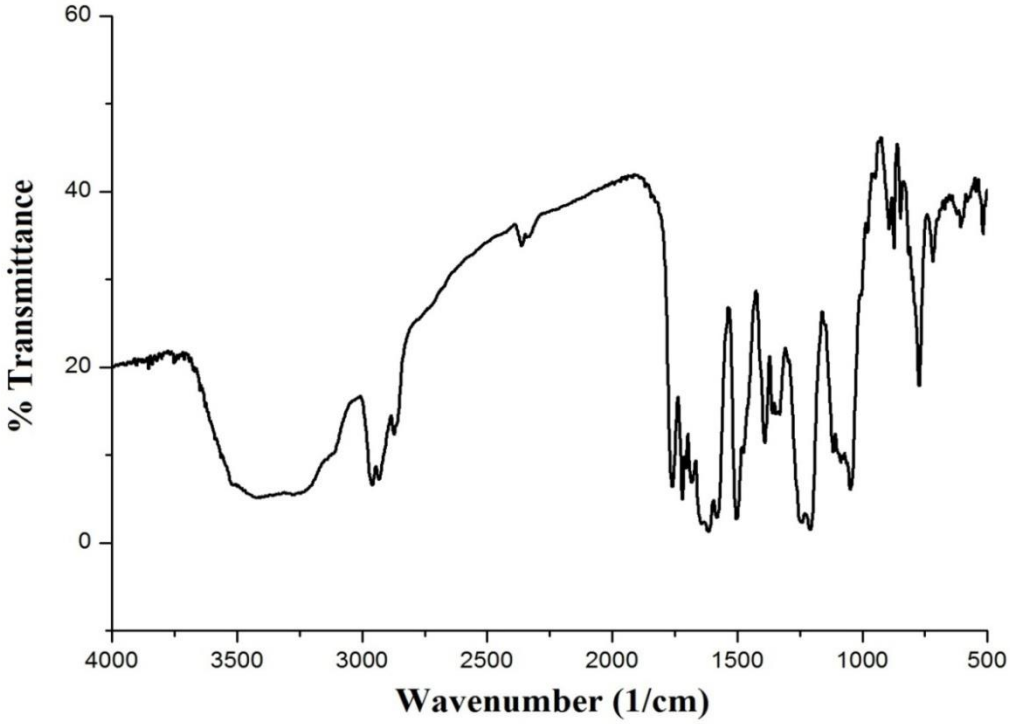

Figure 5.1 FTIR spectrum of drug CAP

Table 5.1 Observed FTIR wavenumber of CAP scanned in the spectral region 4000 to 500 cm^{-1}

Functional group	**CAP (cm^{-1})**
O-H stretching	3406
N-H stretching	3111
Pyrimidine carbonyl stretching	1722
C-F stretching	1047
Tetrahydrofuran stretching	1205

5.1.4 UV Spectrophotometric Analysis of CAP

5.1.4.1 Determination of λ_{max}

Absorption maxima of CAP in phosphate buffer solution (PBS) (pH 6.8) and hydrochloric acid media (0.1 N, pH 1.2) observed on UV spectrophotometer is exhibited in Figures 5.2 and 5.3, respectively. The scanning process was done between 200-400 nm. Both the spectra

showed prominent and distinctive peak at 239 nm, thus chosen as a maximum absorptive peak.

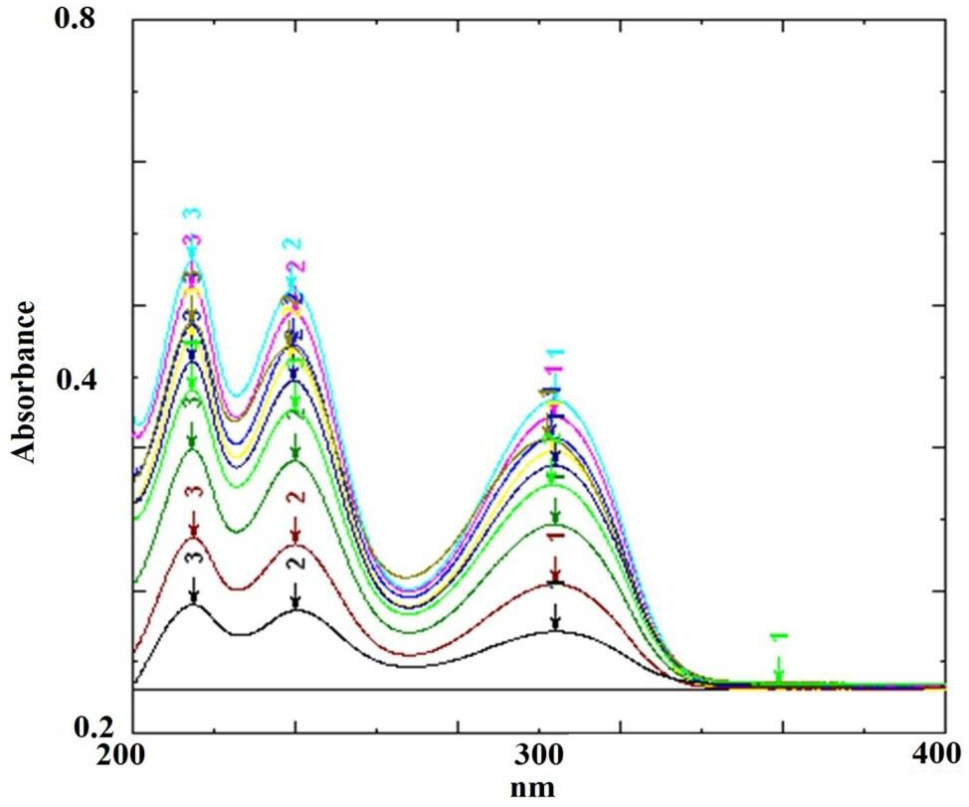

Figure 5.2 UV spectrum of CAP in 0.1 N HCl

(Numbers 1to 3 in above spectrum indicate peak numbers)

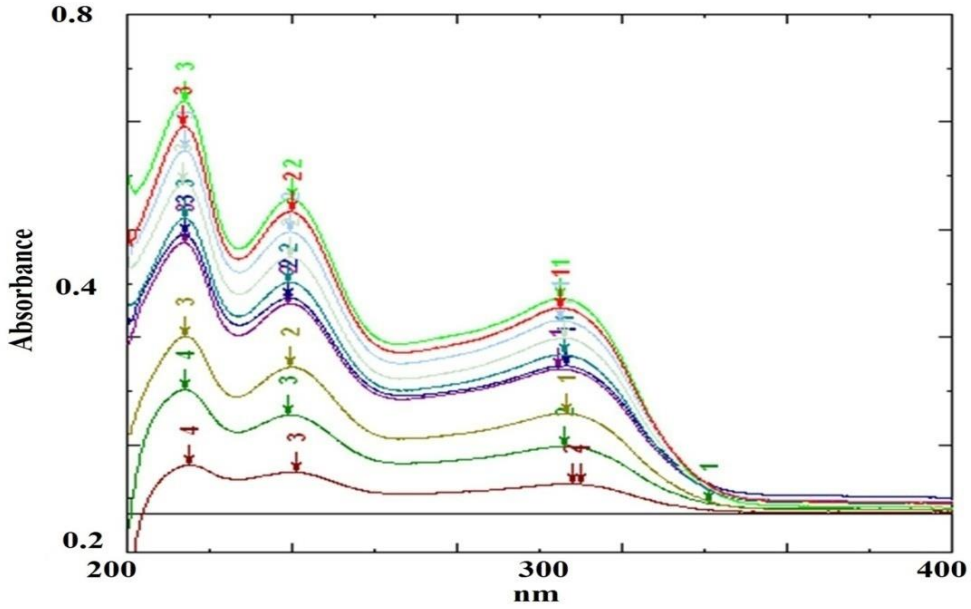

Figure 5.3 UV spectrum of CAP in pH 6.8 PBS

(Numbers 1to 4 in above spectrum indicate peak numbers)

5.1.4.2 a) Standard calibration curve

Standard calibration curve of pure drug CAP was plotted between absorbance and concentration by observing the readings on UV- visible spectrophotometer at a fixed wavelength of 239 nm. All standard solutions of the drug in two media 0.1N HCl (pH 1.2) and PBS (pH 6.8) were prepared in the range of 10-60 µg/mL). A straight line with co-relation coefficient (R^2) value of 0.99 was obtained as shown in Figures 5.4 and 5.5 respectively.

b) Solubility

The solubility of CAP was found to be 25.21 ± 2.9 mg/mL in PBS pH 6.8 and 14.4 ± 1.3 mg/mL in 0.1 N HCl of pH 1.2; (each solubility data is represented as mean ± S.D. n=3)

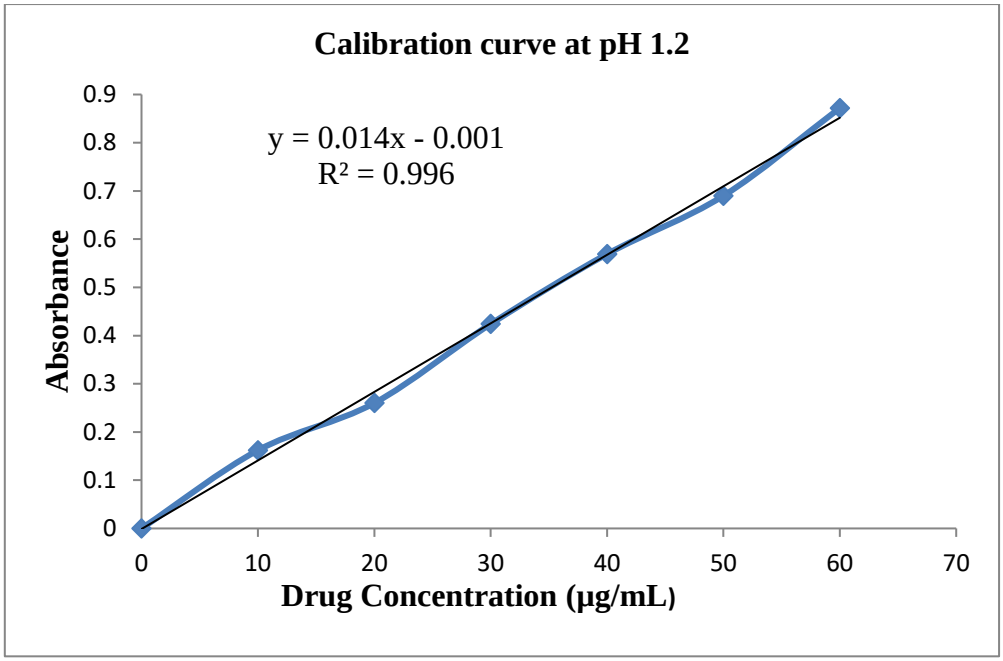

Figure 5.4 Standard calibration curve of CAP in 0.1 N HCl pH 1.2

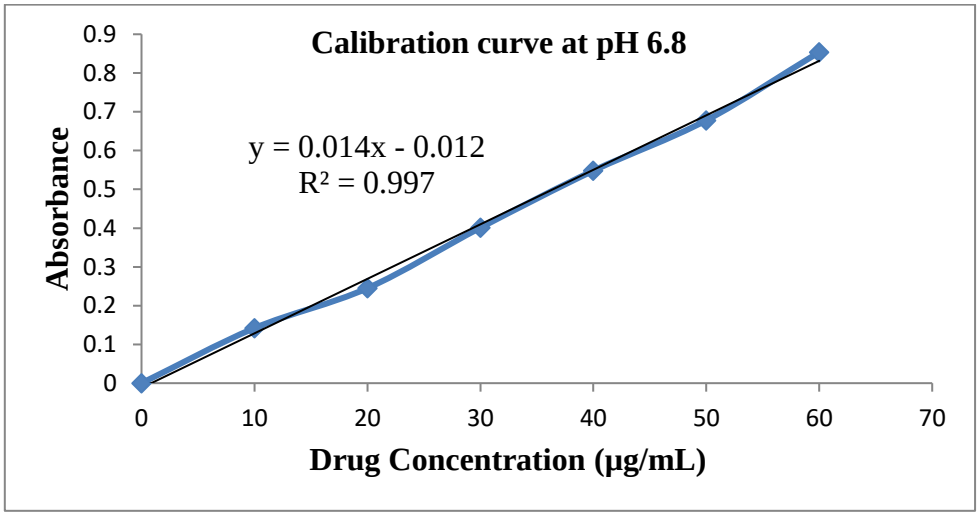

Figure 5.5 Standard calibration curve of CAP in phosphate buffer pH 6.8

5.1.5 HPLC analytical method development of CAP in plasma

According to ICH guideline Q2 (R1) aim of analytical method development is to show that it is suitable for its intended application and would accurately and precisely demonstrate the concentration of unknown samples [Guideline, 2005]. Method validation was performed using Phonomenex C-18 column as the stationary phase and methanol and phosphate buffer (pH 6.8) as mobile phase at flow rate 1 mL/min in isocratic mode. Methanol and PBS buffer were used in several proportions ranging from 10:90 (v/v) to 70:30 (v/v). Tailing was observed when PBS amount was higher than methanol. However, on increasing the proportion of methanol,peak of the CAP became regular. The peak was observed perfectly symmetric in the proportion of methanol and water of 70:30 (v/v). Figure 5.6 shows chromatogram of CAP in plasma at retention time 5.546 min at 232 nm.

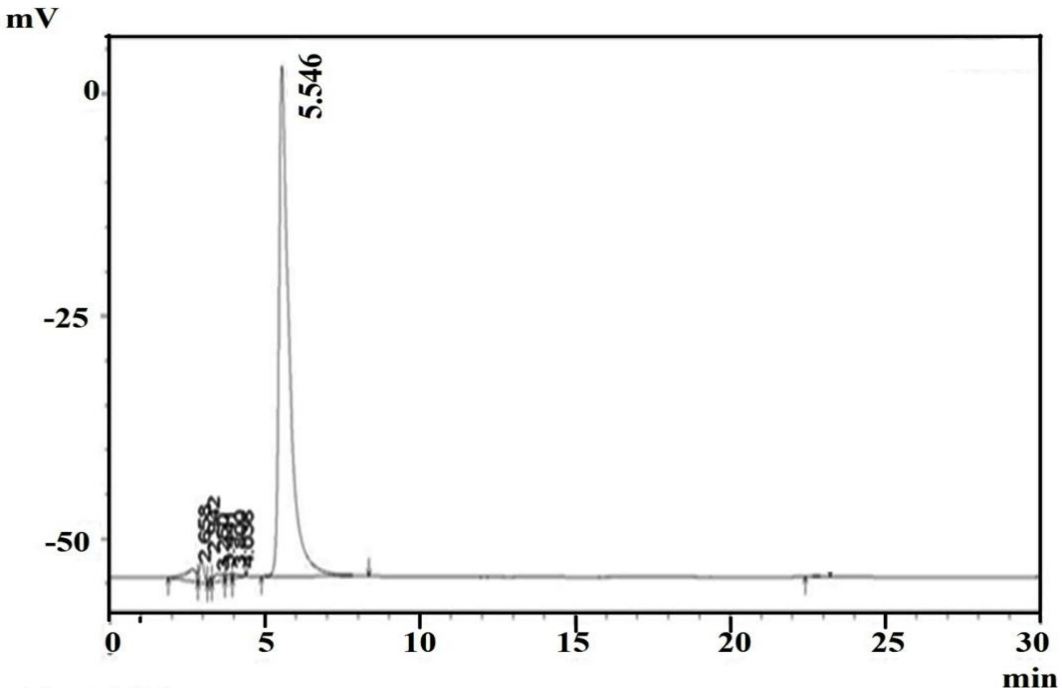

Figure 5.6 Chromatogram of pure CAP in plasma

5.1.5.1 Method development

5.1.5.1.1 Linearity and range

Linearity was estimated at six concentrations ranging from 10-250 µg/mL. A graph was plotted between drug concentration at x-axis and peak area at y-axis resulting into a linear graph (Figure 5.7) with the regression equation and correlation coefficient (R^2) mentioned below:

$$y = 46782x - 12139 \; and R^2 = 0.990 \text{Equation (5. 1)}$$

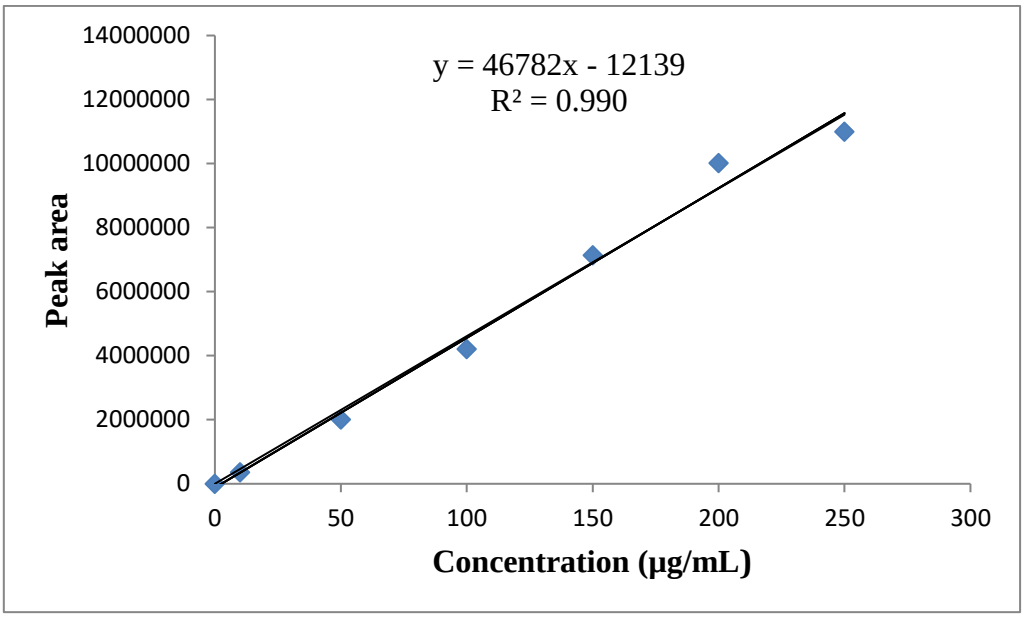

Figure 5.7 Result of linearity

5.1.5.1.2 Precision

The precision of an analytical validation method indicates extent of closeness of the method validation result to the true value. It was performed to observe intra-day and inter-day variability in calibration curves of the drug. The precision of both, intra-day precision (repeatability) and intermediate precision (inter-day precision) was estimated by repeating the experiment in triplicate on the same day and the three different days, respectively to ensure the reproducibility. The study was performed by injecting 6 replicates of 3 concentrations and

the data obtained are shown in Table 5.2. The result of the precision was expressed as % Relative Standard Deviation (%RSD). In both cases i.e. repeatability and inter-day precision, the % RSD was below 15% thus, reveals the method to be reproducible and satisfactory.

Table 5.2 Repeatability and inter-day precision and recovery of the process

Concentration (µg/mL)	**Intra-day Mean ± S.D.**	**RSD (%)**	**Recovery (%)**	**Inter-day Mean ± S.D.**	**RSD (%)**	**Recovery (%)**
10	10.19± 0.70	6.4	101.9	7.22± 0.68	9.41	72.2
150	151.53±0.99	0.65	101.02	148.54±0.95	0.06	99.02
250	252.65±0.93	0.36	101.06	249.57±0.94	0.37	99.82

S.D. = Standard deviation

5.1.5.1.3 Limit of detection (LOD) and Limit of quantitation (LOQ)

The LOD and LOQ for the present study wereestimated from the SD of y-intercept and slope of the calibration curve at levels approximating LOD and LOQ. The values of LOD and LOQ were found to be 0.01 µg/mL and 0.025 µg/mL, respectively[Zufıa et al., 2004].

5.1.5.1.4 Conclusion

The proposed method for the estimation of CAP in plasma was found to be accurate, precise and sensitive. The method was quick and easy to generate useful pharmacokinetic data in time. The results of linearity, precision, recovery LOD and LOQ proved the method to be feasible. Also, the retention time of 5.54 min allows estimation of a large number of samples in a short period of time.

Part I

5.2 Development of Locust bean gum (LBG) and Sodium alginate (NaAlg) based Calcium ion (Ca^{2+}) cross-linked Interpenetrating Polymeric Network (IPN) loaded with Capecitabine (CAP); (F-1)

5.2.1 Fractional Factorial Design (FFD)

FFD for the first time was introduced in 1942 by Fisher while performing an agricultural experiment. Initially, FFD was not supposed to be the powerful and effective design in medicine and health science but later, in the era of biopharmaceutical arena it emerged out as a new exploratory study for organic synthesis and pharmaceutical developments [Morrison, 2005]. Being a fraction of full factorial design, it is an efficient method in reducing a number of experimental trials necessary for a screening study. The fraction is important especially when the researcher aims at identification of the critical factors influencing the response of the system. In the present work 5 most critical independent variables viz. (A) polymer ratio; (B) amount of cross-linker; (C) stirring speed; (D) dropping distance and (E) needle gauze were selected from RA study and were investigated (labelled as 'high' on basis of RPN score mentioned in Table 4.2.). Applying 2^5 full factorial design at two levels high (+1) and low (-1), would result into 32 experiments. However, use of 2^{5-2} fractional factorial design generated small runs of 8 experimental trials. The independent variables with their high and low levels are presented in Table 4.3. Finally, based on Pareto charts the most important factor was selected as shown in Figure 5.8.

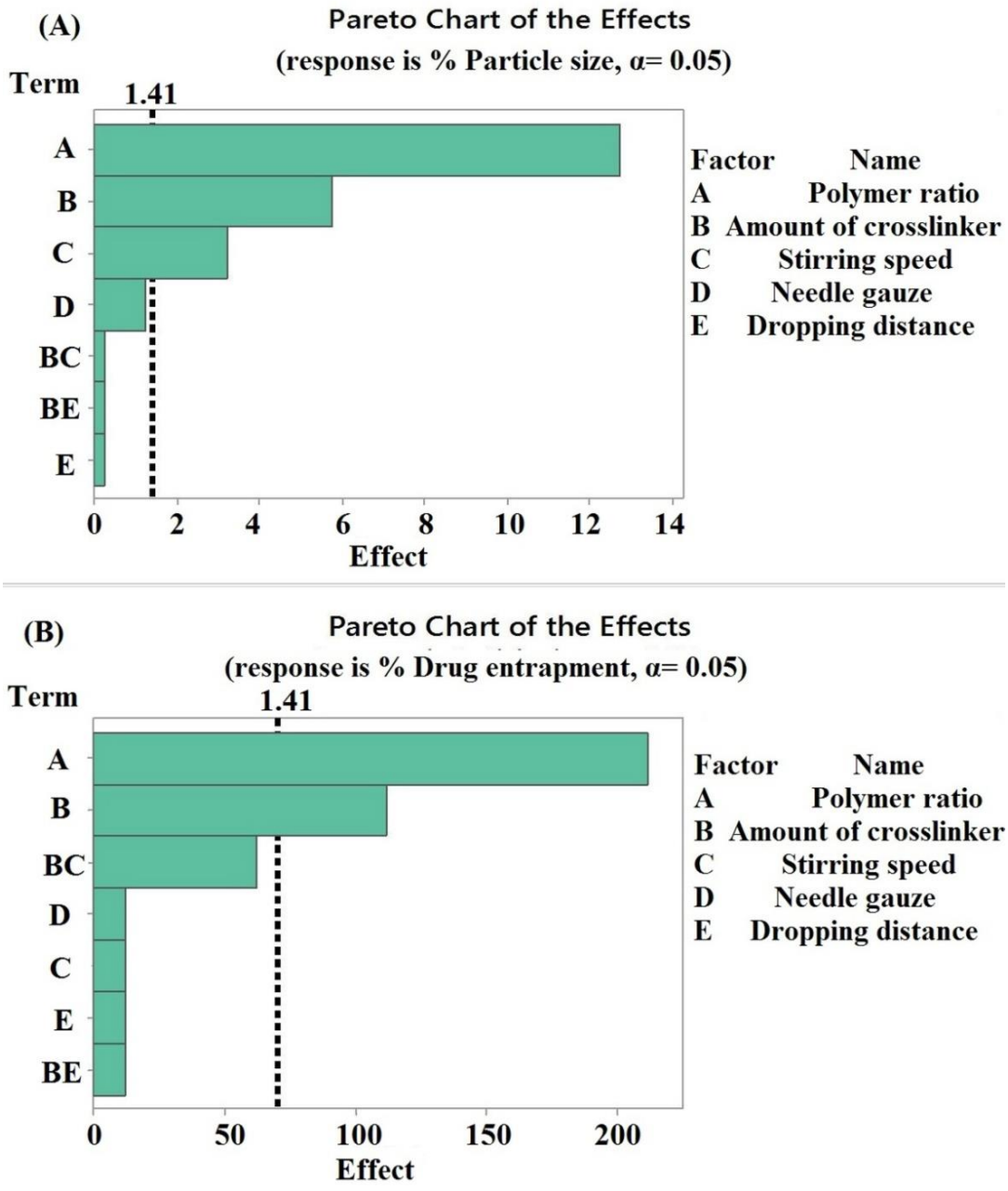

Figure 5.8 Identification of critical factors by Pareto chart

5.2.2 Optimization and statistical analysis

The optimization using Box-Behnken Experimental Design generated a design matrix of 15 experimental runs comprising the test or independent variables i.e. polymer ratio (A), amount of cross-linker (B) and stirring speed (C) with their measured response value termed as particle size (Y_1) and %drug entrapment (Y_2) is illustrated in Table 5.3. Based on the result of BBD experimental batches, an optimized batchcontainingpredicted and experimental values with its level of constraint for the responses is exhibited in Table 5.4. The entire study of optimization process was done with the help of software Minitab-17®. The study was based on one- way Analysis of Variance (ANOVA). Both the responses, particle size and drug entrapment were fitted into different models and the best fit model was selected by considering significant p- values, regression coefficient (R^2) value, Fisher's (F) value and lack of fit value, presented in Table 5.4. For best fitting of the model, value of R^2 as minimum 80% is considered to be desirable [Garg and Prasad, 2016], whereas large F-value indicates large variation in response and p-value lower than 0.05 (< 0.05) indicates the model to be statistically significant [Maran et al., 2015].Further, the three-dimensional response surface plot and two-dimensional contour plots generated shown in Figure 5.9 were also useful in the interpretation of independent variables on responses.

Table 5.3 Box- Behnken experimental design matrix showing the experimental values of responses for the development of Divalent ion cross-linked CAP encapsulated IPN microbeads.

Batch no.	CAP (mg)	LBG: NaAlg (%w/v)	Cross-linker (%w/v)	Stirring speed (rpm)	[a]Particle size (µm) ± S.D.	[a]Drug entrapment (%) ± S.D.
1	50	3:1	2	75	836.50±1.2	81.29±0.7
2	50	1:3	3	100	326.53±4.7	71.43±0.5
3	50	1:1	2	100	675.90±6.8	79.89±1.6
4	50	1:1	4	100	642.89±2.7	84.43±1.1
5	50	1:1	2	50	685.56±9.3	80.28±2.1

6	50	3:1	3	50	829.90±1.7	87.23±3.2
7	50	1:1	3	75	516.70±4.4	78.92±0.1
8	50	3:1	3	100	703.00±8.2	84.78±3.7
9	50	1:1	3	75	521.12±7.2	81.32±2.4
10	50	1:3	2	75	508.12±1.1	69.21±0.9
11	50	3:1	4	75	742.50±3.7	88.73±3.2
12	50	1:3	3	50	494.37±4.8	72.83±0.3
13	50	1:3	4	75	351.05±3.6	75.36±1.8
14	50	1:1	3	75	673.48±2.6	77.46±3.7
15	50	1:1	4	50	689.65±2.9	81.78±2.3

[a]Mean ± SD; n=3

Table 5.4 Independent and dependent variables with their level and constraints

Levels				
Factors	**Low (-1)**	**Medium (0)**	**High (+1)**	**BBD results**
A= Polymer ratio (%w/v)	1:3	1:1	3:1	LBG:NaAlg (1:1)
B= Cross-linker (%w/v)	2	3	4	4
C= Stirring speed (rpm)	50	75	100	100

Dependent Factors	**Constraint**	**Predicted value**	**[a]Experimental value**
Y_1= Particle size (μm)	Minimum	493.76	494.37 ± 1.4
Y_2= Drug entrapment (%)	Maximum	81.46	81.39±2.9

[a]Mean ± SD; n=3.

Table 5.5 ANOVA for the selected model

Dependent Factors	R^2	Adjusted R^2	Predicted R^2	F-value	p-value	Remarks
Particle size (μm)	99.97%	97.89%	95.68%	54.69	0.033	Significant
Drug entrapment (%)	95.51%	95.59%	87.42%	28.77	0.007	Significant

5.2.2.1 Influence of independent factor on particle size

The particle size of the CAP loaded IPN microbeads ranged from 326.53±4.7μm to maximum 836.50±1.2μm. The polynomial equation generated by response surface analysis given below interprets the influence of independent variables on particle size.

Y_1= 1357 + 0.771A – 411B -11.3 C- 0.000368 A^2 + 62.1 B^2 + 0.0656 C^2 + 0.063 AB +0.00164 AC – 0.37 BCEquation(5.2)

From equation 5.2, it can be predicted that among all the model terms A, B, and Conly polymer blend (A) showed a positive coefficient. This suggests that particle size increased on increasing the polymer blend amount. Further, the highest coefficient value of cross-linker (B) suggested that it showed the most significant effect on the particle size which decreased with increasing the amount of cross-linker (B). In the case of the mutual effect of independent factors such as polymer blend (A), cross-linker (B) and stirring speed (C), they all exhibited their significant effect on the particle size. Figure 5.9 clearly depicts the influence of independent factors on particle size by response surface plots and contour plots.

5.2.2.2 Effect of an independent factor on % drug entrapment

The % Drug entrapment of CAP loaded IPN microbeads obtained,varied in the range from 69.21±0.9% to 88.77±3.2%. The polynomial equation generated for the % drug entrapment is given below

Y_2= 81.4+ 0.0508 A+ 6.30 B- 0.412 C- 0.000025 A^2+ 0.97 B^2 + 0.00223 C^2 +0.00129 AB – 0.000042 AC - 0.0304 BCEquation (5.3)

Equation 5.3 shows that % drug entrapment increased with increase in both the model terms A (polymer blend) and B (cross-linker amount). This can be justified by the viscous nature of the polymers and a good binding property of cross-linker with the polymers. Further, the independent factor stirring speed (C) havinga negative coefficient indicated that it had an antagonistic effect on the % drug entrapment. The effect of an independent factor on % drug entrapment is shown by response surface plots and contour plots in Figure5.9.

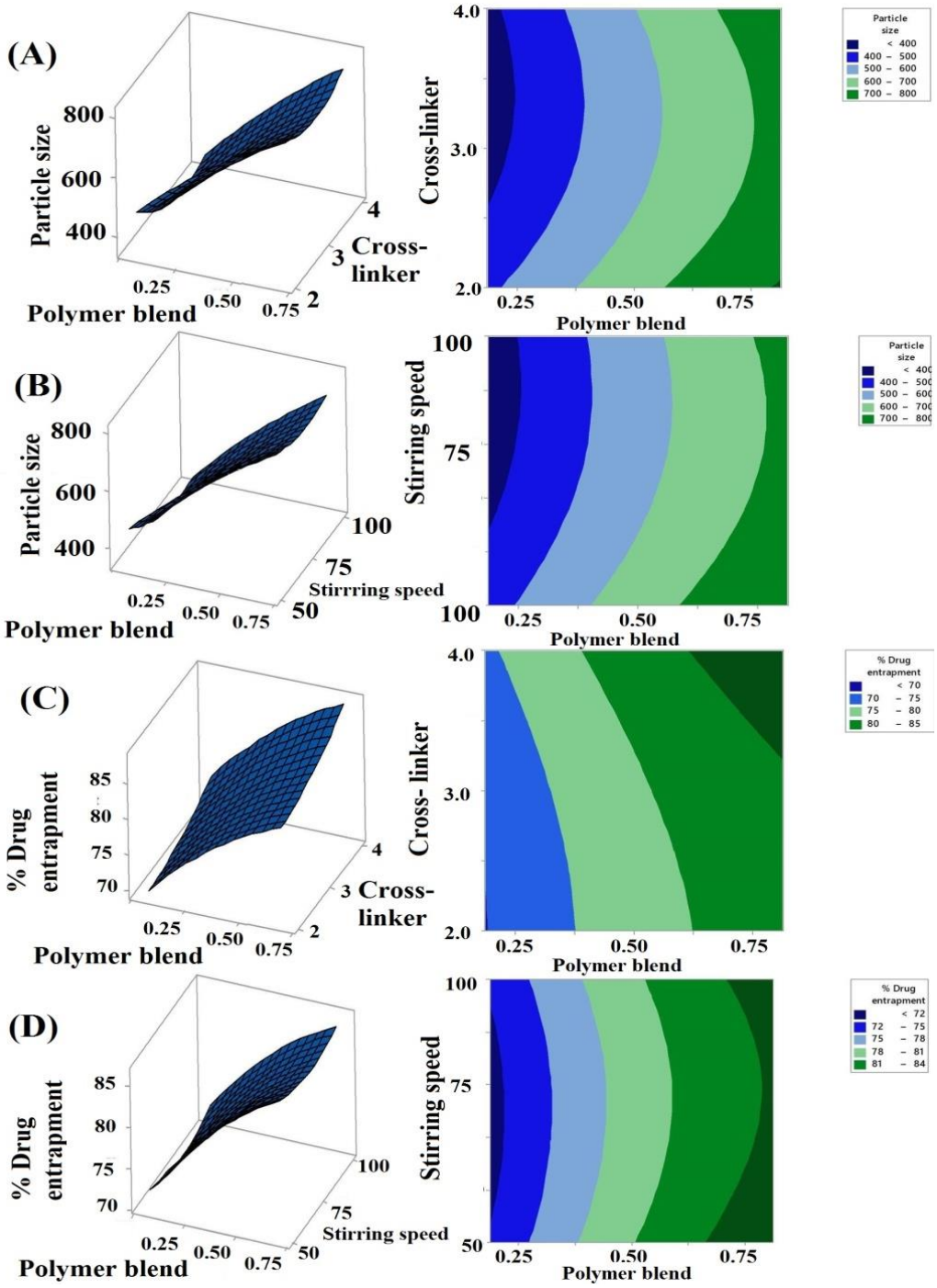

Figure 5.9 Three dimensional response surface and Two dimensional contour plot showing effect of cross-linker and stirring speed on particle size (A, B) and % drug entrapment (C, D)

5.2.3 Characterization

5.2.3.1 Determination of particle size

5.2.3.1.1 Optical microscopy

Optical microscopy is suitable for counting and characterizing the particles of 1µm or greater. Size of the microbeads when observed through microscope was observed in the range from 326.53 ± 4.7 µm to 836.50 ± 1.2 µm. The image of the particles investigated through an optical microscope is shown in Figure 5.10

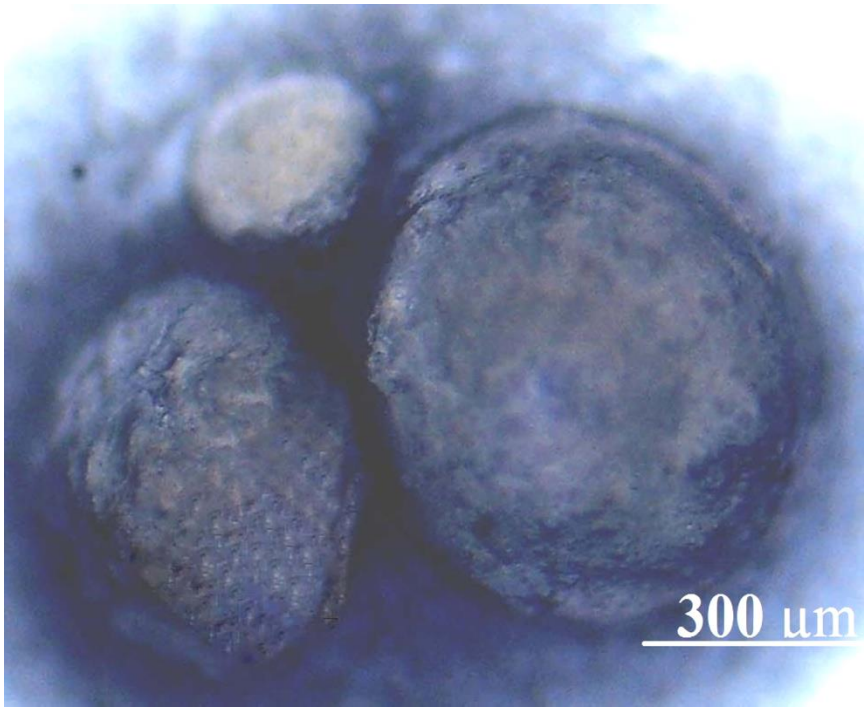

Figure 5.10 Electron microscopic image of CAP loaded Ca^{2+}cross-linked IPN microbeads

5.2.3.1.2 Scanning Electron Microscopy (SEM)

Formed IPN microbeads were also observed by SEM instrument. The photomicrographic image of SEM illustrated in Figure 5.11, shows that the prepared beads were spherical in shape with a somewhat uneven surface that may be due to the gelation process that resulted in crumbled and irregular surface during drying of the microbeads.

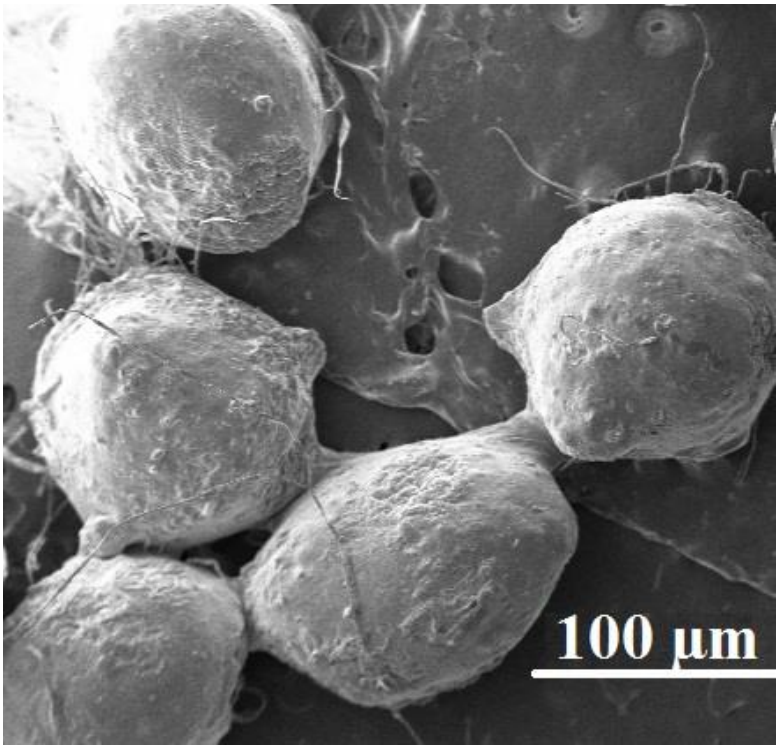

Figure 5.11 Scanning electron microscopic image of CAP loaded Ca^{2+}cross-linked IPN microbeads

5.2.3.2 Energy Dispersive X-ray (EDX)

The elemental composition of formed microbeads studied by EDX is exhibited in Figure 5.12. Few amounts of calcium chloride (Ca = 6.47%, and Cl = 8.51%) was observed on the surface of the microbeads which was washed later with distilled water to avoid its adsorption. Presence of trace amount of sodium (Na = 0.52%) indicated a successful exchange of calcium with guluronic unit of sodium alginate. Apart from Ca, Cl and Na, the other elements observed during analysis were C = 45.34% and O = 39.16%.

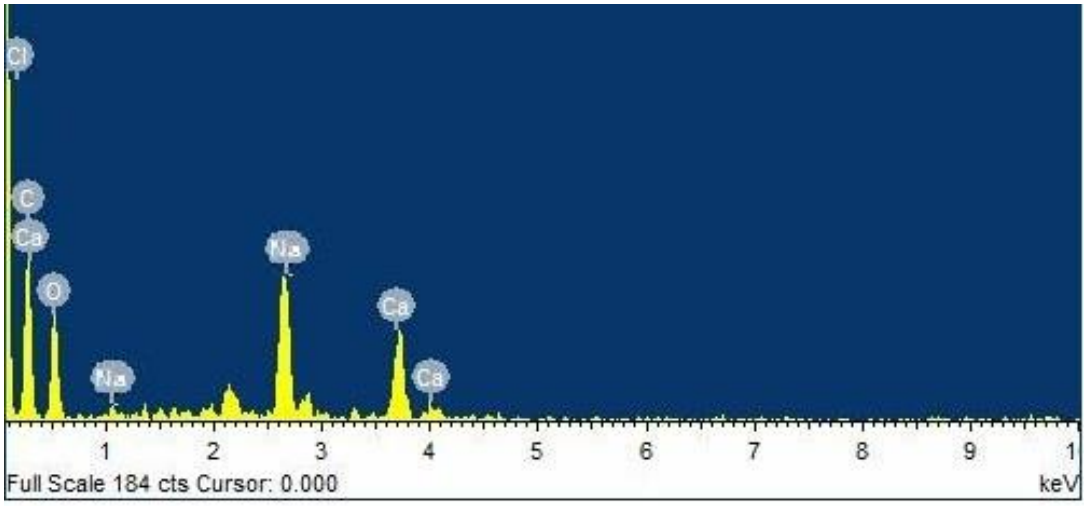

Figure 5.12 Elemental composition of the CAP loaded Ca^{2+}cross-linkedIPN microbeads

5.2.3.3 Drug entrapment (%)

The polymeric mixture and the cross-linker both played a synergistic role in influencing the % drug entrapment. The formulations batch no 1, 6, and 11involving more LBG and less NaAlg showed high drug entrapment. It was due to the more hydrophilic nature of NaAlg than LBG. Both polymers are polysaccharide and are composed of mannose (hydrophobic) and galactose units, (hydrophilic) possessing certain Mannose/Galactose (M/G) value that governs the solubility of polymer i.e. higher the mannose value more the polymer will be hydrophobic[Dionísio and Grenha, 2012a]. The reported M/G value of LBG and NaAlg are 4 and 0.53 respectively, thus, LBG shows limited solubility [Kaity et al., 2013b]. Therefore, with an increase in the part of LBG, the size of the IPN microbeads got increased hence; possibility to entrap more amount of drug was also increased. Another factor that enhanced the % drug entrapment was cross-linker concentration. Increasing calcium chloride concentrationfrom2% w/v to 4% w/v, % drug entrapment was found 81.29% ± 0.7 (Batch no.1) and 88.73%±3.2 (Batch no. 11). Ca^{2+} possess a good affinity for NaAlg and chelates easily [Sikorski et al., 2007]. The mechanism of chelation involves association of the

scattered MM or GG blocks with D-mannuronic acid (M) and L-guluronic acid (G) residues of NaAlg [Donati et al., 2005]. This conjugation helped the polymer blend to hold the drug firmly and prevented the oozing of the drug in the external media thus, drug entrapment increased. The third independent factor, stirring speed exhibited a slight effect on % drug entrapment [Upadhyay et al., 2018a].

5.2.3.4 *In vitro* drug release study

The *in vitro* drug release study was conducted for optimized formulation in pH 1.2 medium for 2 h followed by in pH 6.8 media for remaining 10 h (Figure 5.13). Release of the drug from polymeric microbeads at pH 1.2 was only 12% which was low in comparison to pH 6.8, where microbeads showed drug release of 95%. The variation in the release pattern as a function of pH is based on the concept of swelling. At low pH 1.2, polymeric microbeads remained compact due to the protonation of the carboxyl group present in the polymeric chains that lead to the less swelling causing less amount of drug release through polymeric networks. However, at high pH 6.8, the beads showed burst release followed by sustained release. Burst effect during drug release was observed due to free drug present on the surface of microbeads that released immediately when in contact with release media. After certain time release of drug from the microbeads was slowed down, because of the low glass transition temperature of amorphous CAP that turns viscous in contact with water and being further entrapped within the viscous polymeric network the drug leached out slowly thus, showed a sustained release pattern [Meulenaar, 2013]. The release kinetic data obtained was fitted into release kinetic models of zero order, Higuchi, Hixson-Crowell, and first-order model which showed regression coefficient (R^2) as 0.79, 0.94, 0.79 and 0.92 respectively. Among all the R^2 value for Korsmeyer- Peppas model was found to be maximum i.e. 0.98 with exponential constant (n) 0.7. The value of n as 0.7 further indicated the anomalous

diffusion of drug from the microbeads that may be combined effect of swelling and diffusion controlled.

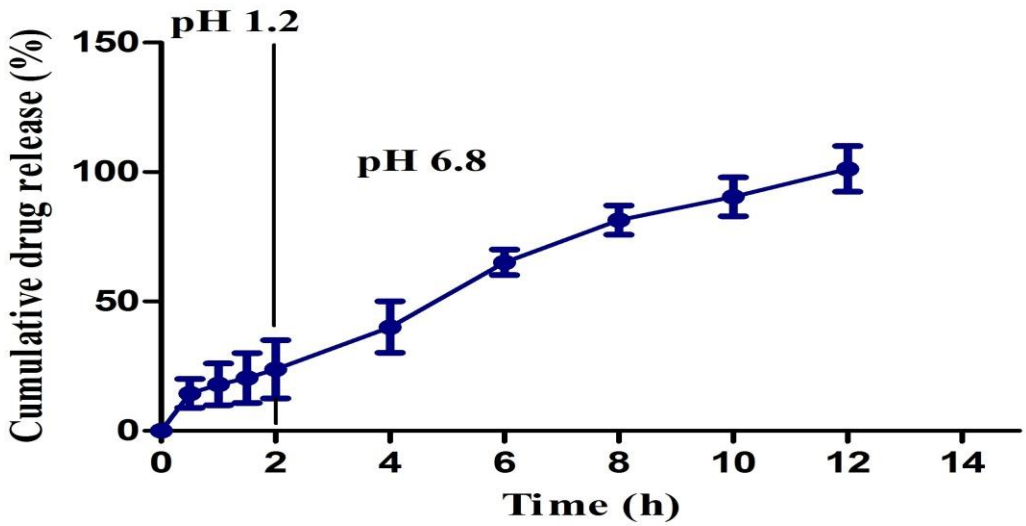

Figure 5.13*In vitro* drug release profile ofCAP loaded Ca^{2+} cross-linkedoptimized IPN microbeads (vertical bars represent mean± S.D. n=3)

5.2.3.5 Stability study

According to ICH guideline Q 1A (R2) shelf life of a pharmaceutical product is defined as "the time during which a drug product characteristics remains within the approved specification, provided that it is stored under the same condition as defined on the label of container" [Capen et al., 2012]. The stability study was conducted to observe their potential to withstand the variable environmental condition. Particle size, % drug entrapment and total drug content of the microbeads kept at different storage condition were estimated and compared with the freshly prepared sample (Table 5.6). No significant change ($p>0.05$) was

observed. Finally, based on the total drug content shelf life was calculated as a function of time (month) at which total drug content reaches to 90%. The shelf life of IPN microbeads was found to be 17.51 months, 10.13 months and 5.55 months at refrigeration, room and a high temperature of storage as respectively shown in Figure 5.14.

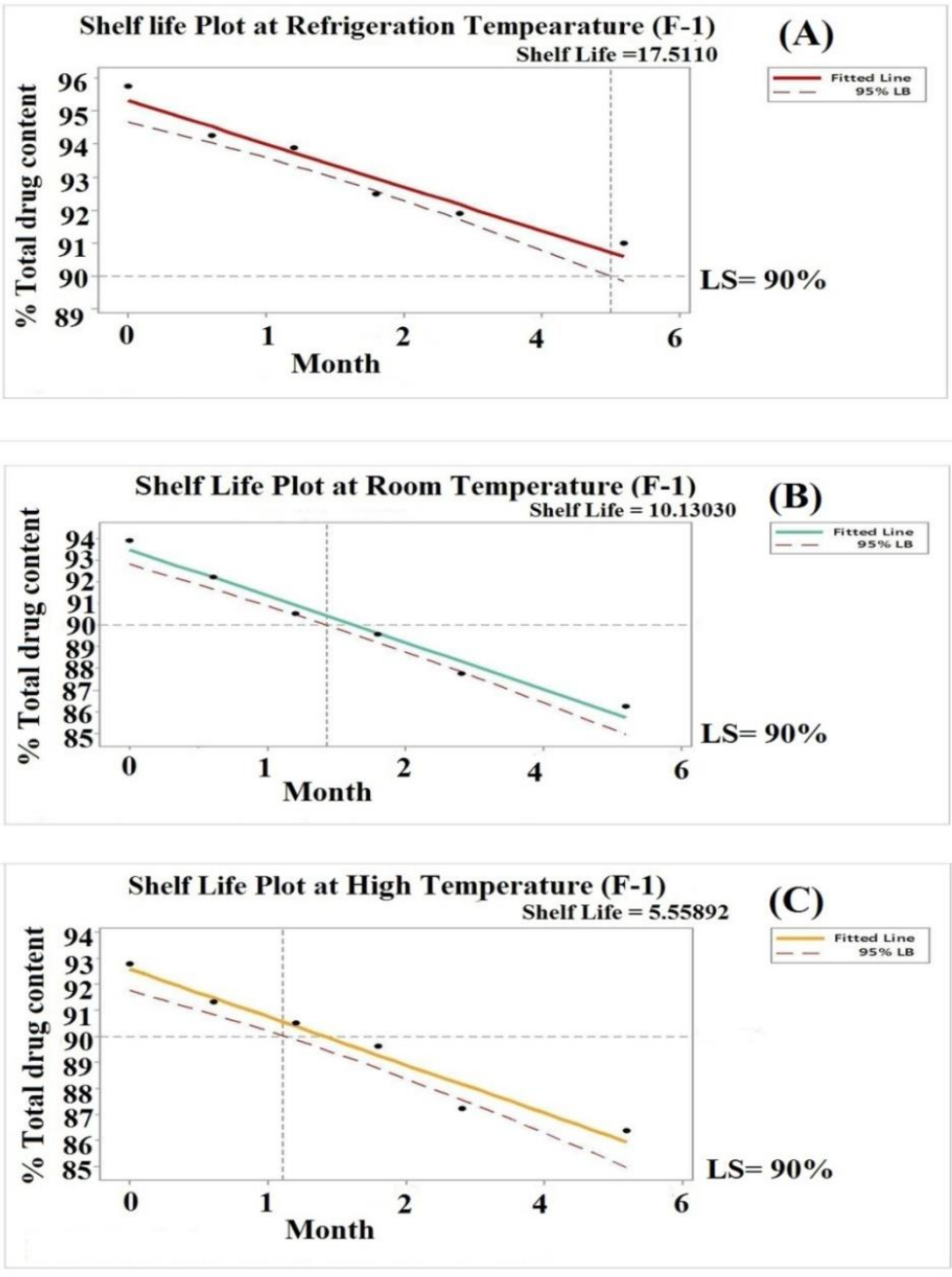

Figure 5.14 Shelf -life plots of an optimized batch ofCa^{2+} cross-linked IPN microbeads stored at (A) refrigerated temperature, (B) room temperature and (C) high temperature with the lower specification (LS) set at 90%

Table 5.6 Results of stability study of divalent ion cross-linked IPN microbeads stored for 6 months

At the end of 6 months				
Parameters	**[a]Fresh prepared sample**	**[a]Refrigeration Temperature**	**[a]Room Temperature**	**[a]High Temperature**
Particle size (µm)	495.72 ± 1.5	494.65 ± 1.0	493.58 ± 1.4	491.83 ± 2.2
Drug entrapment (%)	80.92 ± 1.1	79.83 ± 2.5	78.59 ± 1.4	77.95 ± 2.3
Total drug content (%)	96.76 ± 1.7	95.56 ± 2.9	93.92 ± 1.6	92.77 ± 2.3

[a]Mean ± SD; n=3.

Part II

5.3Development of Locust bean gum (LBG) and Sodium alginate (NaAlg) based Aluminum ion (Al^{3+}) cross-linked Interpenetrating Polymeric Network (IPN) loaded with Capecitabine (CAP); (F-2)

5.3.1Fractional Factorial Design

For the preparation of IPN microbeads, several parameters such as type of polymer, amount of polymer, concentration of cross-linker, type of cross-linker, stirring speed dropping distance, curing time, needle gauze etc. were taken into consideration during optimization process in order to get an optimum and best result. Among all these parameters the selection of critical factor was based on scoring of the factors also known as Risk Priority Number (RPN) obtained by RA study, Failure Mode Effective Analysis (FMEA) shown in Table 4.4. All the possible CMAs and CPPs scoring 10 or > 10 i.e. polymer ratio (A), amount of cross-linker (B), curing time (C), Needle gauze (D) and Dropping distance (E) were selected and further used in FFD for screening purpose (Table 4.5). Finally using Pareto chart (Figure

5.15) the factors crossing the reference line, were considered as the most critical factor and were utilized in final optimization study termed as BBD that generated 15 experimental runs and helped in achieving the best-optimized formulation.

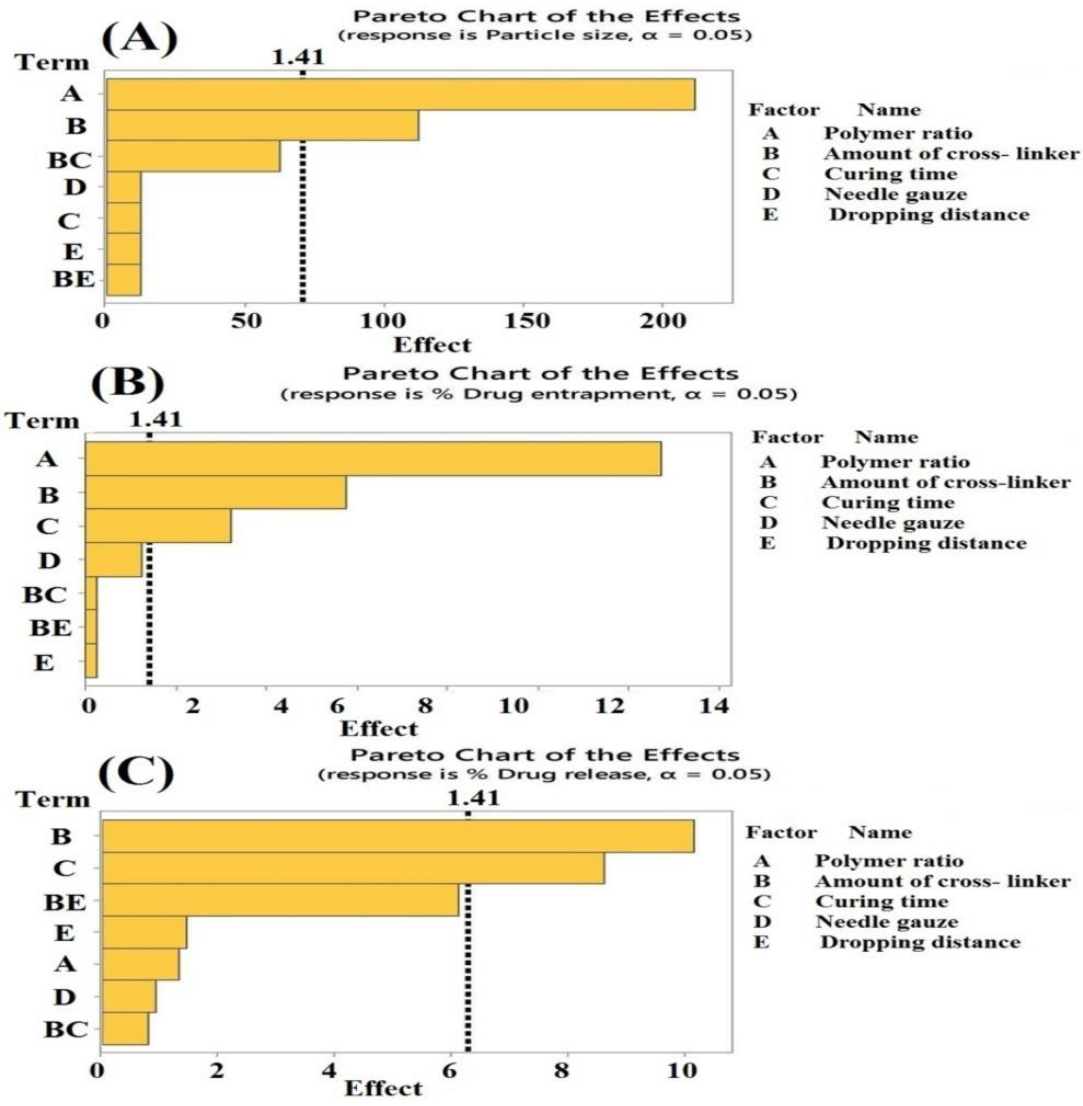

Figure 5.15 Identification of critical factors by Pareto chart

5.3.2 Optimization and statistical analysis

After the screening of significant factors made by FFD, optimization was performed by BBD using Minitab software 17® (Table 5.7).

Table 5.7 Box- Behnken experimental design matrix showing the experimental values of responses for the development of trivalent ion cross-linked CAP encapsulated IPN microbeads.

Batch no	CAP (mg)	LBG:NaAlg (% w/v)	$AlCl_3$ (%w/v)	Curing time (h)	[a]Particle size (µm)	[a]Drug entrapment (%)	[a]Drug release (12 h) (%)
1	50	1:3	2	1.5	370.20± 1.4	59.33± 0.7	86.32±2.4
2	50	1:3	3	1.0	364.77± 2.1	61.21±0.2	75.87±2.7
3	50	3:1	3	2.0	537.65± 4.6	82.39±1.1	70.54±1.1
4	50	3:1	3	1.0	535.86± 3.8	85.89±3.7	76.21±2.6
5	50	1:1	3	1.5	436.71± 6.1	67.01±3.2	73.11±2.2
6	50	1:3	3	2.0	359.19±7.5	58.29±2.5	71.75±1.5
7	50	1:3	4	1.5	354.68± 4.3	60.57±0.1	61.75±1.9
8	50	3:1	2	1.5	540.12± 1.9	83.78±2.6	85.44±2.8
9	50	1:1	2	1.0	450.16± 2.5	69.61±1.9	90.18±2.2
10	50	1:1	2	2.0	442.62± 4.4	66.18±0.4	80.34±2.7
11	50	1:1	3	1.5	438.83± 5.6	70.64±2.3	72.96±2.3
12	50	1:1	4	2.0	432.11± 1.5	71.49±1.5	55.76±1.6
13	50	3:1	4	1.5	530.45± 2.3	84.65±2.6	60.45±1.1
14	50	1:1	3	1.5	434.08± 3.9	72.14±2.8	69.42±2.8
15	50	1:1	4	1.0	429.31± 5.7	74.51±0.5	62.34±2.4

[a]Mean ± SD; n=3.

The experimental design had 3 levels, 3 factors and 3 Centre points. The independent factorsselectedwere amount of polymer (A), amount of cross-linker (B), and curing time (C) whereas particle size (Y_1), % drug entrapment (Y_2) and % drug release (Y_3) were chosen as a response. Independent variable with their levels (high, medium, and low) and set constraints are described in Table 5.8. The suitable quadratic model was selected on basis of statistical

data p-value, regression coefficient (R^2) value, Fisher's (F) value and lack of fit value, exhibited in Table 5.9. Further, forthe best suited model, two-dimensional surface plots and three-dimensional contour plots (Figure 5.16) were also generated showing the effect of independent factors on dependent variables. Finally, abest-optimized batch was selected based on constraint of dependent variable and used for all physical, *in vitro* and *in vivo* characterization.

Table 5.8 Independent and dependent variables with their level and constraints.

Levels				
Factors	**Low (-1)**	**Medium (0)**	**High (+1)**	**BBD results**
A= Polymer ratio (%w/v)	1:3	1:1	3:1	LBG:NaAlg (1:1)
B= Cross-linker (%w/v)	2	3	4	2
C= Curing time (h)	1	1.5	2	1

Dependent Factors	**Constraint**	**Predicted value**	**[a]Experimental value**
Y_1= Particle size (µm)	Minimum	453.52	457.92 ± 1.6
Y_2= Drug entrapment (%)	Maximum	71.24	74.11 ± 3.1
Y_3= Drug release (%)	Maximum	89	90.23 ± 2.1

[a]Mean ± SD; n=3.

Table 5.9 ANOVA for selected quadratic model

Dependent Factors	**R^2**	**Adjusted R^2**	**Predicted R^2**	**F-value**	**p-value**	**Remarks**
Particle size	99.97%	99.92%	99.78%	54.69	0.0001	Significant
% Drug entrapment	98.24%	95.08%	87.07%	28.77	0.0001	Significant
% Drug release	99.18%	97.7%	95.7%	66.97	0.0001	Significant

5.3.2.1 Influence of independent factor on particle size (Y_1)

Particle size (Y_1) of formed IPN microbeads ranged from 354.6μm ± 4.3 to 540.12μm ± 1.9. The mathematical equation (Equation 5.4) generated for the particle size clearly depicts that the polymeric ratio, LBG:NaAlg (A) playeda positive role in enhancing the particle size whereas the factored amount of cross-linker (B) exhibitedan antagonistic effect on the response particle size.

$Y_1 = 394.6 + 0.1228\ A - 40.1\ B + 0.000185\ A^2 + 0.753\ B^2 + 0.00585\ AB$

Equation (5.4)

5.3.2.2 Influence of independent factor on particle size (Y_2)

The % Drug entrapment (Y_2) for the prepared formulations varied from 58.29 % ± 2.5 to 85.89 %± 3.7. The polynomial equation generated for the above-mentioned response is expressed in Eq.5.5. From the equation, it can be said that all the three factors i.e. polymer ratio (A); the amount of cross-linker (B) and curing time (C) exhibited their significant role in either increasing or decreasing the entrapment of drug within the polymeric matrix. The independent factor (A) and (B) showed synergistic effect whereas factor (C) exhibited negative influence towards the entrapment of drug.

$Y_2 = 57.3 + 0.0223\ A + 0.55\ B - 5.5\ C + 0.000029\ A^2 + 0.33\ B^2 + 0.76\ C^2 - 0.00116\ AC + 0.20\ BC$ Equation (5.5)

5.3.2.3 Influence of independent factor on % drug release (Y_3)

The response % drug release (Y_3) ranged from 55.76% ± 1.6 to 86.32%± 2.4 and was highly influenced by the factor (B) amount of cross-linker and factor (C) curing time. The Equation 5.6 clearly illustrates that both these factors had antagonistic effect thus, decrease in the % release of drug.

$Y_3 = 84.1 - 19.38\ B - 30.1\ C + 1.363\ B^2 - 7.19\ C^2 + 0.32\ BC$ Equation (5.6)

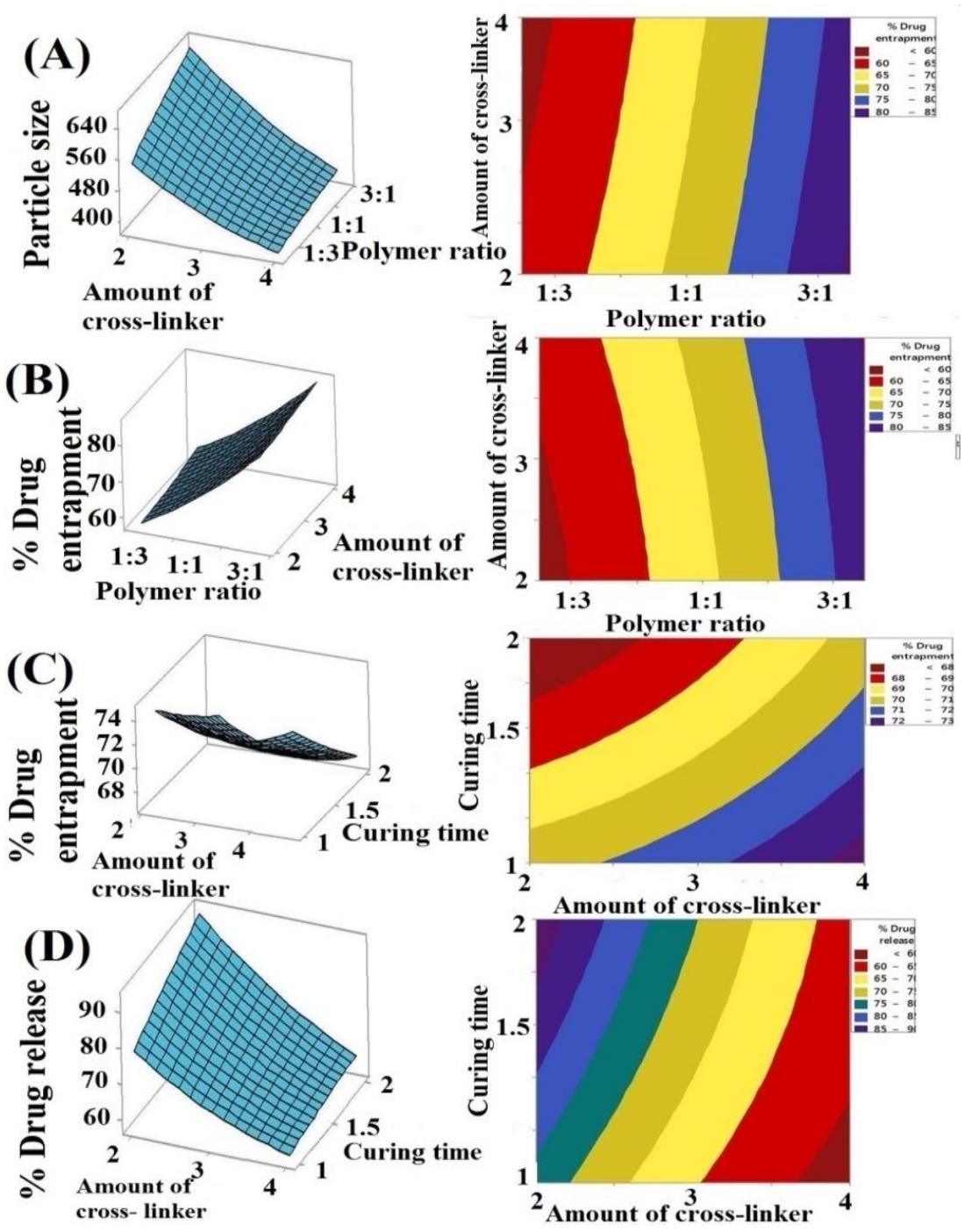

Figure 5.16 Two dimensional and three dimensional contour plots showing the effect of independent factors on responses (a) particle size; (b) and (c) for % drug entrapment and (d) for % drug release.

5.3.3 Characterization

5.3.3.1 Determination of particle size

5.3.3.1.1 Optical electron microscopy

The average particle size of developed IPN microbeads measured by digital microscope, varied from 354.6μm ± 4.3 to 540.12μm ± 1.9 and appeared spherical in shape with a regular surface. The photo micrographic image of microbeads is presented in Figure 5.17.

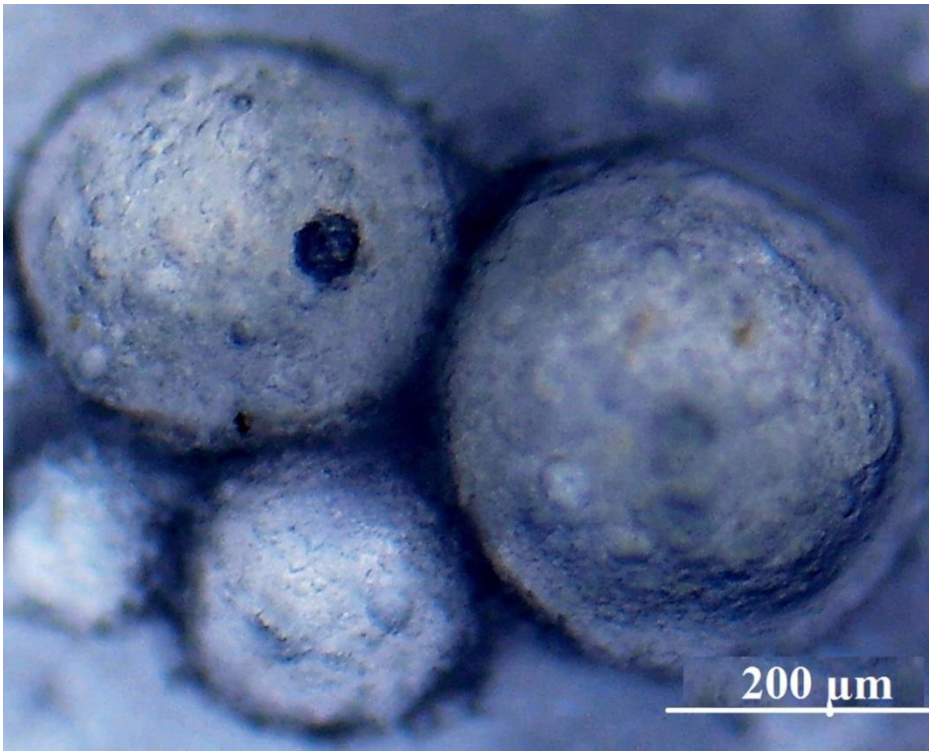

Figure 5.17 Electron microscopic image of Al^{3+}cross-linked IPN microbeads

5.3.3.1.2 Scanning electron microscopy (SEM)

SEM image of the CAP loaded IPN microbeads observed at 100X magnification (Figure 5.18) was spherical in shape with a beaked protrusion at the top without any agglomeration.

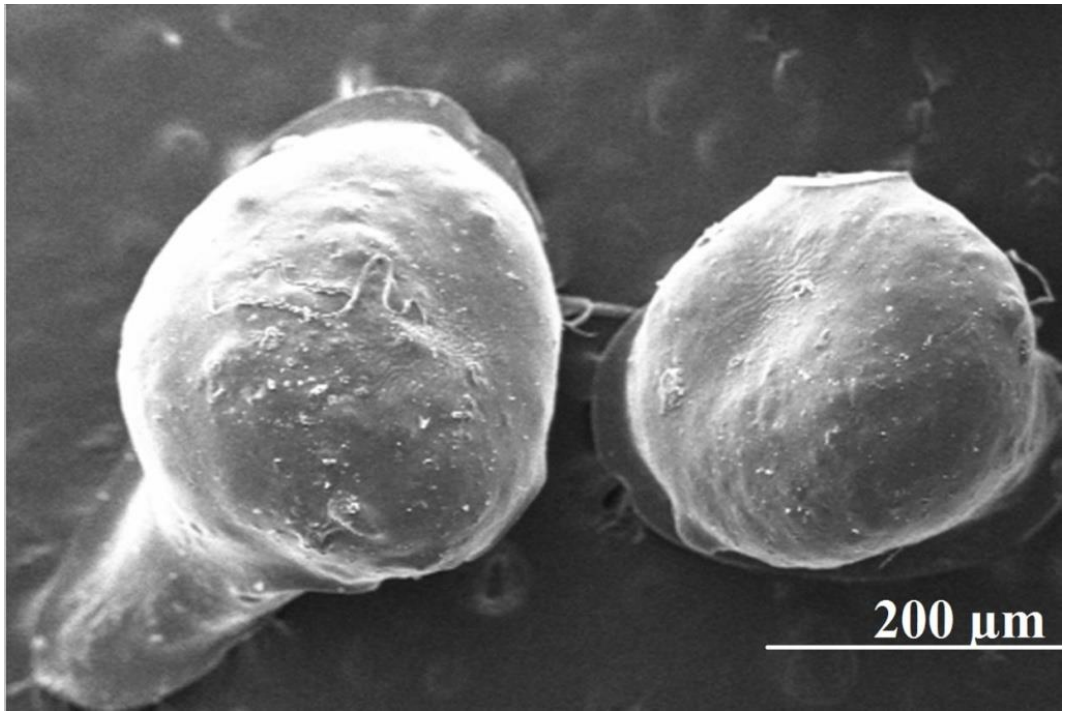

Figure 5.18 Scanning electron microscopic image of CAP loaded Al^{3+}cross-linked IPN microbeads.

5.3.3.2 Energy dispersive X-ray (EDX)

Estimation of elements present in CAP loaded trivalent cross-linked IPN microbeads through EDX study is exhibited in Figure 5.19. Detection of aluminum (Al = 6.79%) and chloride (Cl = 16.26%) on surface of the microbeads is indicating its successful adsorption. Presence of a minimal quantity of sodium (Na = 0.58%) showing complete exchange of Al^{3+} with three guluronic units of sodium alginate. Besides these, the other elements observed were carbon (C = 25.03%) and oxygen (O = 51.34%).

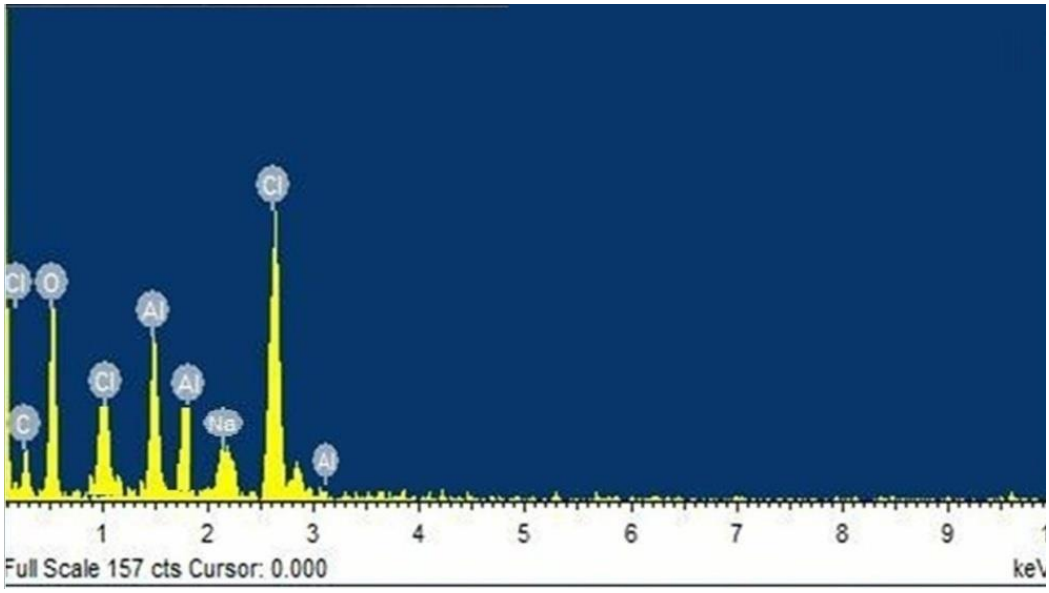

Figure 5.19 Elemental analysis of the Al^{3+}cross-linked IPN microbeads

5.3.3.3 Drug entrapment (%)

The drug entrapment (%) of CAP encapsulated within IPN microbeads varied from 59.33 ± 0.7 to 85.89 ± 3.7. From the results as presented in Table 5.7, it can be inferred that the formulation batch composed of more part of LBG in the polymeric blend and more amount of cross-linker showed high % DE. The result was due to high viscous nature of LBG than NaAlg that imparted dense and aggregated texture to the polymeric blend leading to the less diffusion of drug into media [Pollard et al., 2008]. Another factor that supported an increase in the drug entrapment was firm cross-linking of Al^{3+} with NaAlg. Al^{3+}contains three positive charge that attaches strongly with a guluronic unit of NaAlg and forms rigid cross-linked network thus more drug was entrapped within IPN microbeads [Nokhodchi and Tailor, 2004].

5.3.3.4 *In vitro* drug release study

In vitro drug release study of CAP from optimized formulation was performed for 2 h in acidic media (0.1N HCl pH 1.2) and remaining 10 h in alkaline media (phosphate buffer pH 6.8) (Figure 5.20). For the first two hours,release of CAP was found to be minimal (about 10%). However, after two hours a notable release (60%) of drug from the formulation was

observed in the first 6 h followed by slow and continuous sustained release till 12 h (90% of drug released at 12 h). Such variation in the release pattern of CAP from prepared microbeads was due to its swelling behavior in the different buffer media. At low pH (pH 1.2), low swelling was observed due to carboxyl functional groups in the network that remained protonated in the acidic media resulted in the rigidly closed network, thus, drug leached slowly from the less swelled beads. At high pH, the same functional group undergoes ionization that resulted into increased osmotic and electrostatic force leading to high drug release [Kikuchi et al., 1997]. However, after some time the drug release was slowed down and showed a sustained release pattern this was due to the low glass transition temperature of amorphous CAP. It is reported that the amorphous CAP converts rapidly into a gel when comes in contact with water that slows down its dissolution [Meulenaar, 2013]. To determine the release kinetics of the optimized formulation, the results obtained were fitted into different models such as zero order, first order, Higuchi, Korsmeyer–Peppas and Hixson–Crowell release kinetics model and on the basis of highest value of R^2 (R^2 =0.952) it was inferred that the optimized formulation followed zero order release kinetics.

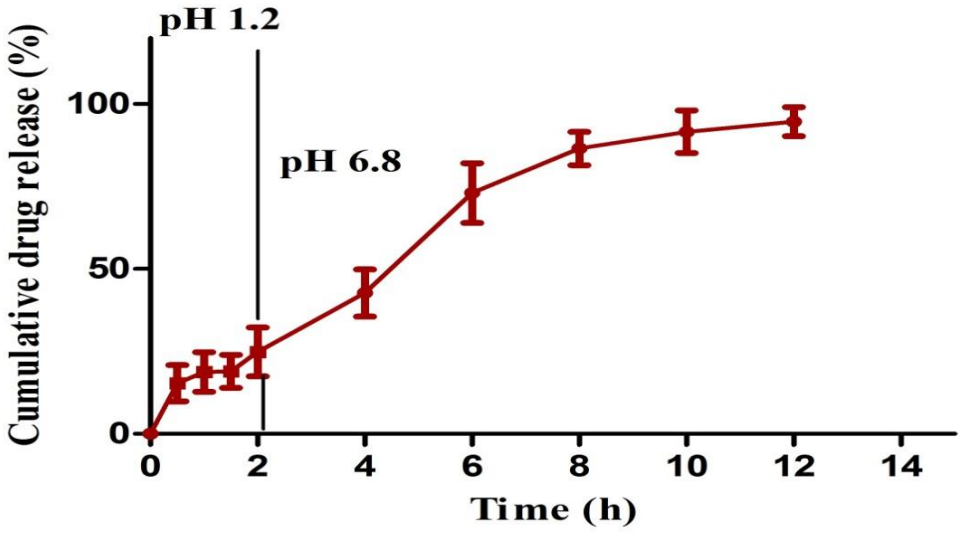

Figure 5.20*In vitro* drug release profile of Al^{3+} cross-linked CAP loaded IPN microbeads (vertical bars represent mean± S.D. n=3)

5.3.3.5 Stability study

Stability study of the optimized batch of trivalent ion cross-linked IPN microbeads performed and compared with the freshly prepared sample for the parameters particle size, % drug entrapment and % total drug content. All the selected attributes showed a non- significant difference ($p > 0.05$) with samples stored at three different conditions (Table 5.10). The calculated shelf life obtained with the help of Minitab-17® were 19.6 months, 14.5 months and 8.2 months at refrigerated, room and high temperature respectively (Figure 5.21)

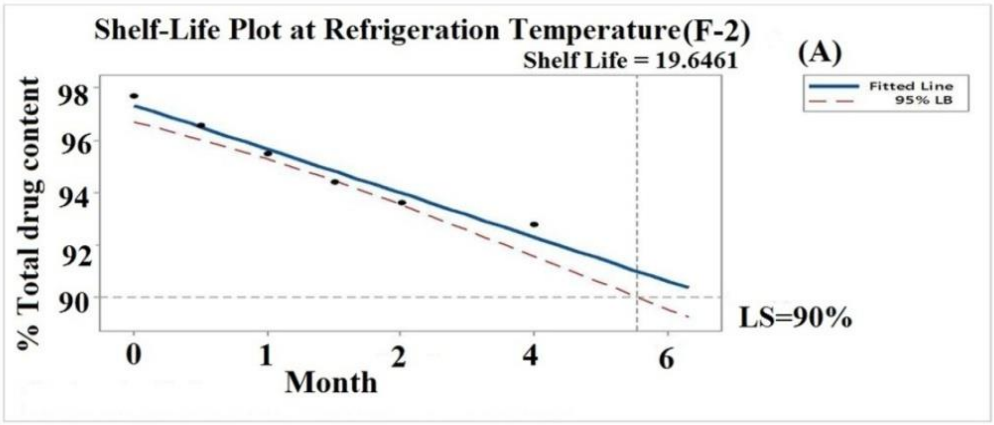

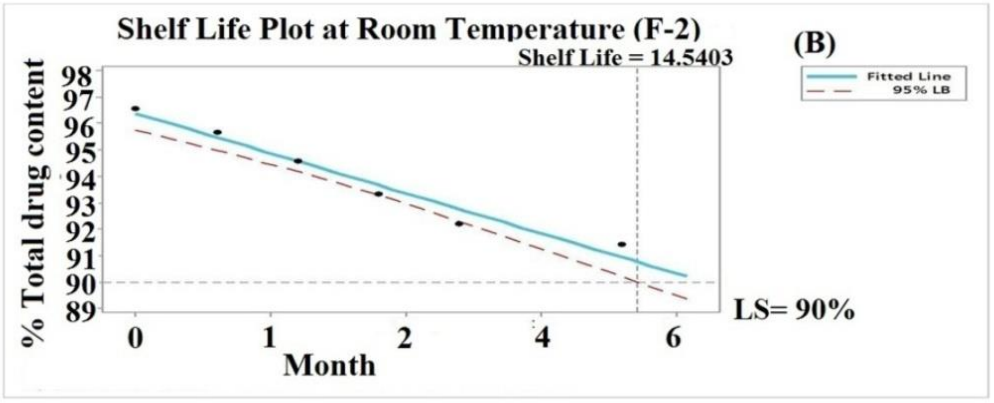

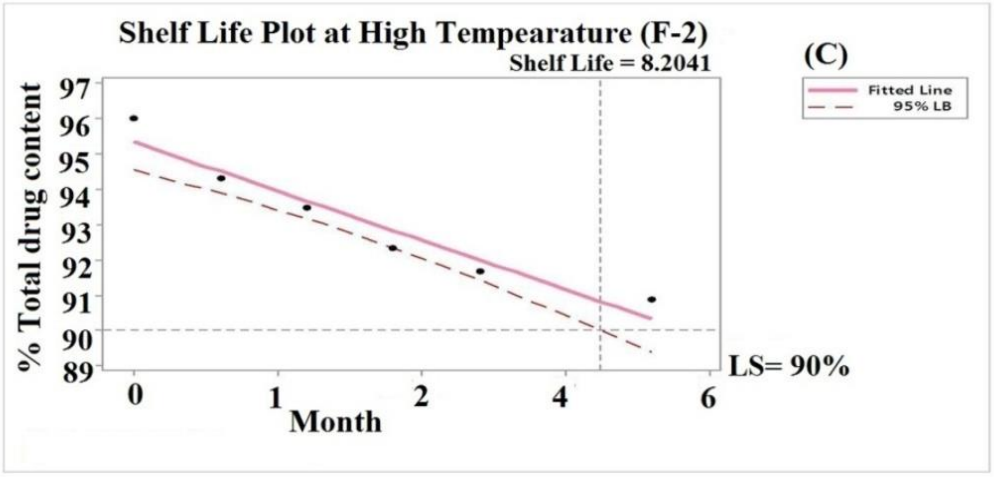

Figure 5.21 Shelf-life plots of optimized of trivalent ion cross-linked IPN microbeads stored at different conditions (A) refrigeration temperature, (B) room temperature and (C) high temperature with lower specification (LS) set at 90%

Table 5.10 Results of stability study of trivalent ion cross-linked IPN microbeads stored for 6 months

At the end of 6 months				
Parameters	[a]**Fresh prepared sample**	[a]**Refrigeration Temperature**	[a]**Room Temperature**	[a]**High Temperature**
Particle size (µm)	460.93 ± 1.2	458.54 ± 1.5	456.33 ± 2.5	455.76 ± 2.8
Drug entrapment (%)	73.89 ± 3.2	72. 93 ± 2.9	71.45 ± 1.8	70.69 ± 2.7
Total drug content (%)	98.89 ± 1.3	97.69 ± 1.8	96.57 ± 1.4	95.99 ± 1.9

[a]Mean ± SD; n=3.

Part III

5.4Development of Locust bean gum (LBG) and Sodium alginate (NaAlg) based Aluminum ion (Al^{3+}) cross-linked buoyant and mucoadhesive Interpenetrating Polymeric Network (IPN) loaded with Capecitabine (CAP); (F-3)

5.4.1Fractional Factorial design

All the critical CMAs and CPPs affecting CQAs during development of buoyant IPN microbeads were considered and subjected to RA study FMEA. Based on risk score i.e. factors scoring > 10 were further subjected to FFD (Table 4.7).Finally, after analyzing the data obtained through FFD, a Pareto chart (Figure 5.22) was generated that in real sense screened the main factors that might actually affect the response during preparation of IPN microbeads.

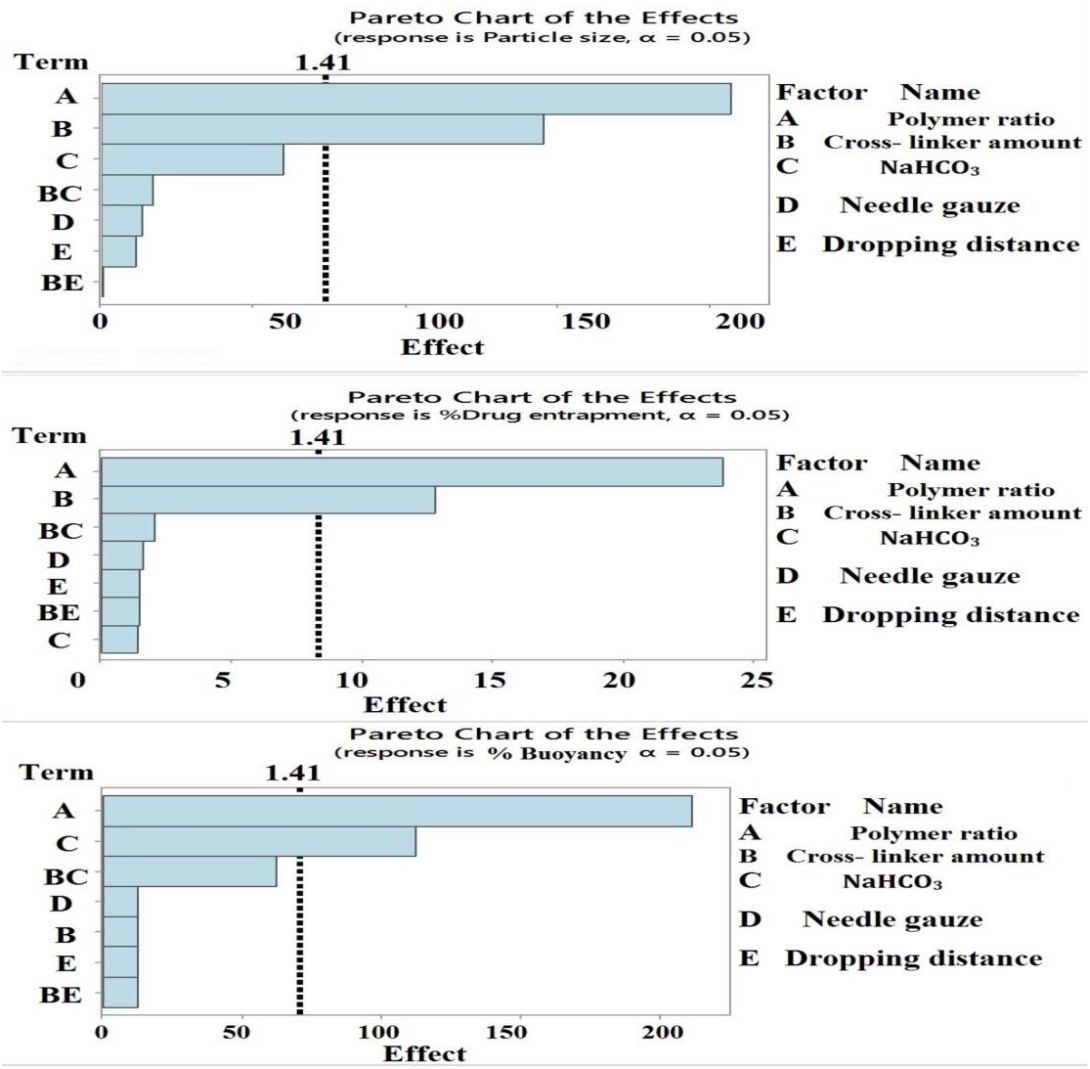

Figure 5.22Identification of critical factors by Pareto chart

5.4.2 Optimization and statistical analysis

Box Behnken Design was utilized for optimization of trivalent ion (Al^{3+}) cross-linked buoyant IPN microbeads. The design was composed of 15 experimental runs carrying 3 independent variables (screened out from FFD) polymer ratio (A), amount of cross-linker and amount of $NaHCO_3$ (C) exhibiting their influence on 3 responses i.e. particle size (Y_1), % drug entrapment (Y_2)and % buoyancy (Y_3) (Table 5.11). The independent factors with their level and set constraints and also the result of thebest-optimizedbatch with their predicted and experimental values are mentioned in Table 5.12 The interaction of the factors with responses were illustrated by means of contour and 3-dimensional plots (Figure 5.23) and the statistical analysis of each responses were done by fitting the data in the model (linear, quadratic and two factor interaction) investigated by ANOVA shown in Table 5.13.

Table 5.11 Experimental plan for the preparation of buoyant cross-linked IPN microbeads

Formulation Batch	Polymer ratio (%w/v)	Cross-linker amount (%w/v)	$NaHCO_3$ Amount (mg)	[a]Particle size (µm)± S.D.	[a]Drug entrapment (%)± S.D.	[a]Buoyancy (%)± S.D.
1	1:1	2	10	434.39± 2.1	72.65± 3.1	60.05±2.5
2	1:3	3	55	350.09± 1.1	61.55± 2.5	85.28±3.1
3	1:1	3	55	428.76± 3.4	76.38± 2.6	72.18±2.7
4	1:1	4	100	418.78± 2.2	80.11± 1.8	79.51±4.5
5	1:3	4	10	336.12± 2.9	64.85± 1.6	82.31±2.6
6	3:1	2	10	541.56± 3.4	88.06± 2.8	40.53±1.9
7	1:3	2	10	357.62± 3.1	57.85± 3.4	80.69±3.2
8	1:1	3	55	426.87± 2.7	74.89± 1.2	74.98±2.8
9	3:1	3	10	527.59± 2.5	91.23± 3.2	45.64±2.9
10	1:1	2	55	432.29± 2.6	74.25± 1.5	65.71±2.5
11	3:1	4	100	520.05± 1.6	94.69± 2.8	54.62±3.5
12	3:1	3	55	525.31± 2.7	72.19± 2.2	50.38±2.1
13	1:3	3	100	348.51± 3.5	60.02± 1.3	85.66±2.3
14	3:1	3	55	530.45± 2.0	90.75± 1.7	48.04±3.8
15	1:1	4	100	420.48± 2.7	79.59± 1.4	76.58±2.4

[a]Mean ± SD; n=3.

Table 5.12 Optimal parameters with their level, constraints, predicted value, experimental value and summary of ANOVA

Levels				
Factors	**Low (-1)**	**Medium (0)**	**High (+1)**	**BBD results**
A= Polymer ratio (%w/v)	1:3	1:1	3:1	LBG:NaAlg 1:1
B= Cross-linker (%w/v)	2	3	4	2
C= $NaHCO_3$ (mg)	10	55	100	100

Dependent Factors	**Constraint**	**Predicted value**	**[a]Experimental value**
Y_1= Particle size (µm)	Minimum	426.98	402.12 ± 1.9
Y_2= Drug entrapment (%)	Maximum	79.88	82.45 ± 2.5
Y_3= Buoyancy (%)	Maximum	77.54	85.03 ± 1.1 TFT > 10 h

[a]Mean ± SD; n=3.

Table 5.13Summary of the ANOVA

Model	**R^2**	**Adjusted R^2**	**Predicted R^2**	**F-value**	***p*-value**	**Remarks**
Response: Particle size(Y_1)						
Quadratic	0.9998	0.9994	0.9980	2695.98	<0.0001	Significant
Response: Drug entrapment (Y_2)						
Linear	0.9887	0.9856	0.9841	320.06	<0.0001	Significant
Response: % Buoyancy (Y_2)						
Quadratic	0.9945	0.9847	0.9358	101.06	<0.0001	Significant

5.4.2.1 Influence of independent factor on particle size (Y_1)

The quadratic model was suggested for the above response. The model F-value also known as Fisher's F-value 2695.98 indicating it to be significant whereas Lack of fit F- value 20.83 suggesting it as non- significant. The value of the predicted R^2 i.e. 0.9980 is in the reasonable agreement with the adjusted R^2 0.9994 which means the model is adequate to fitthe

experimental data. Further to estimate signal to noise ratio adequate precision of the model is required, which should be greater than 4.In case of particle size, the ratioobtained was 144.369 thus; the model can be used to navigate the design space. The polynomial equation generated for particle size is given below:

$(Y_1) = 426.98 + 89.40\ A - 6.97\ B - 0.7175\ C - 0.3075\ AB - 0.32\ 2\ AC + 0.725\ BC + 12.10A^2 + 0.0562B^2 + 0.07\ C^2$ Equation (5.7)

The coded terms A, B, C, AB, AC, BC A^2, B^2 and C^2 included in the model also helped in the interpretation of relation between independent variable and factors. Among all the coded terms only the polymeric ratio (A) had a positive value indicating a synergistic effect on the particle size whereas the value of amount of cross-linker (C) havinga highest coefficient value of 6.97 had a most significant and antagonistic effect on particle size. A graphical presentation of the effects of variables on the responses is exhibited in Figure 5.24.

5.4.2.2 Influence of independent factor on drug entrapment (Y_2)

A linear model was suggested for the above response. Model F- value of 320.06 implies the model is significant. The Lack of Fit F- value of 0.33 suggested the model non- significant with respect to pure error. The Predicted R^2 of 0.9841 was found in practicable agreement with the Adjusted R^2 of 0.9856. The ratio of 50.536 indicated an adequate signal and suggested the model in navigating the design space. The polynomial equation for drug entrapment is given below:

$(Y_2) = 75.5933 + 15.0575\ A + 3.30375\ B - 0.13375\ C$ Equations (5.8)

The coded model terms A and B have a positive value of coefficient representing a favorable synergistic influence on the drug entrapment while a negative value of C showing an antagonistic relationship. The interaction of independent factors with their responses is shown in Figure 5.23.

5.4.2.3 Influence of independent factor on buoyancy (Y_3)

The quadratic model was suggested for the above response. Model F-value of 101.06 approved the model to be fit and significant. Lack of Fit F-value of 3.11 indicated the model to be non- significant. The value of Predicted R^2 0.9258 was in rational agreement with the adjusted R^2 0.9847. The signal to noise ratio of 33.035 indicated an appropriate signal and proposed the model for navigation of the design space. The polynomial equation for buoyancy is given below:

$(Y_3) = 73.5933 - 9.6025A – 0.5B + 9.45125\ C – 2.1275\ AB – 0.37\ AC + 1.1475\ BC – 9.03167\ A^2 + 1.73083\ B^2 – 6.36167$Equation (5.9)

The positive values of the independent factors A and C coded for polymer ratio and amount of $NaHCO_3$ respectively implies that % buoyancy increased with increase in the amount of $NaHCO_3$ and decreased with the polymer ratio and. The interaction of the terms with responses is shown in Figure 5.23

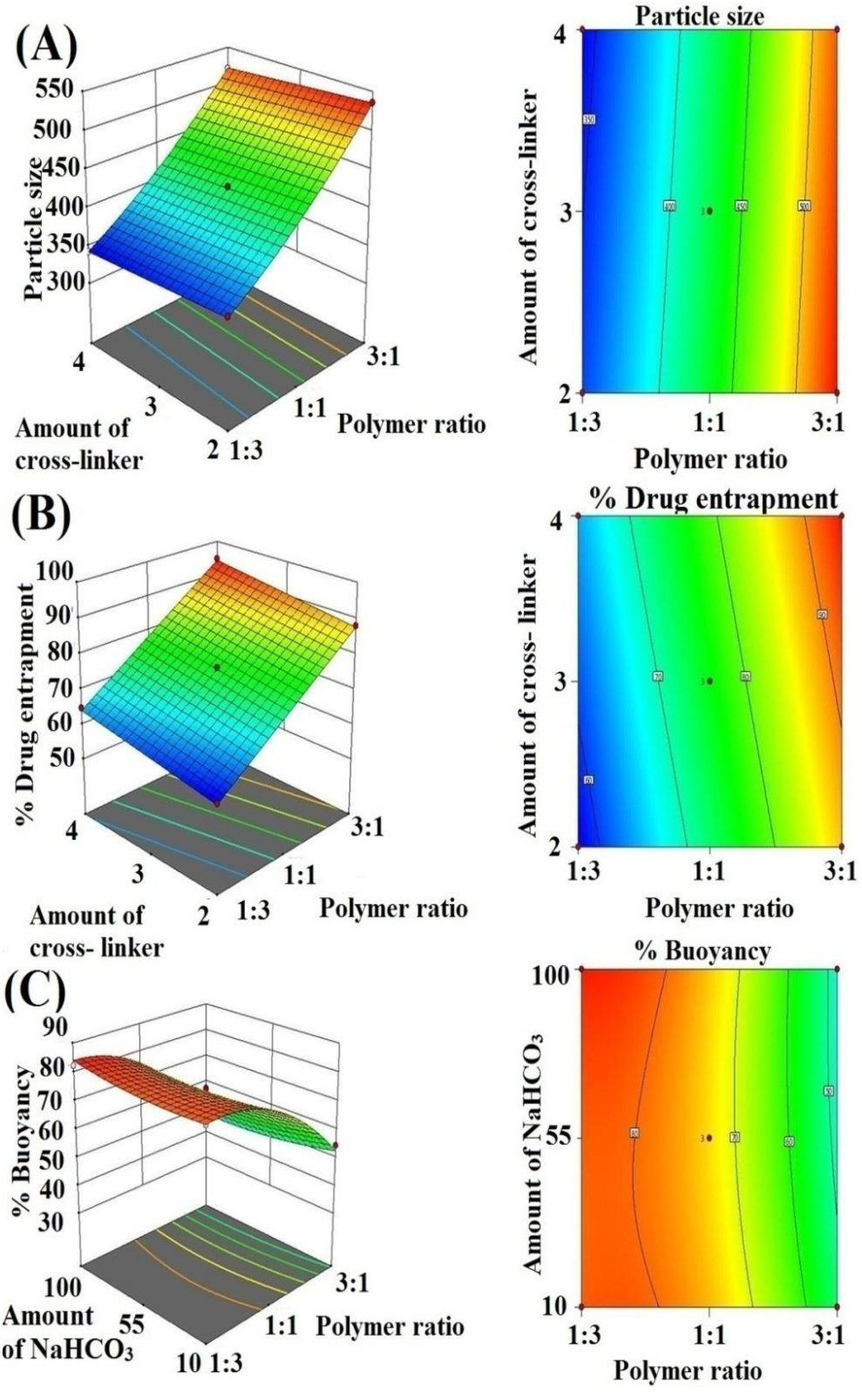

Figure 5.23 Two dimensional and three-dimensional contour plots showing the effect of independent factors on responses (A) particle size; (B) % drug entrapment and (C) % buoyancy.

5.4.3 Characterization

5.4.3.1 Determination of particle size

5.4.3.1.1 Optical microscopy

The microscopic image of the buoyant IPN microbeads observed through an optical microscope is exhibited in Figure 5.24. The size of the microbeads varied in the range from 333.12 ± 2.9 µm to 541.56 ± 3.4 µm and was found to be spherical and of regular shape.

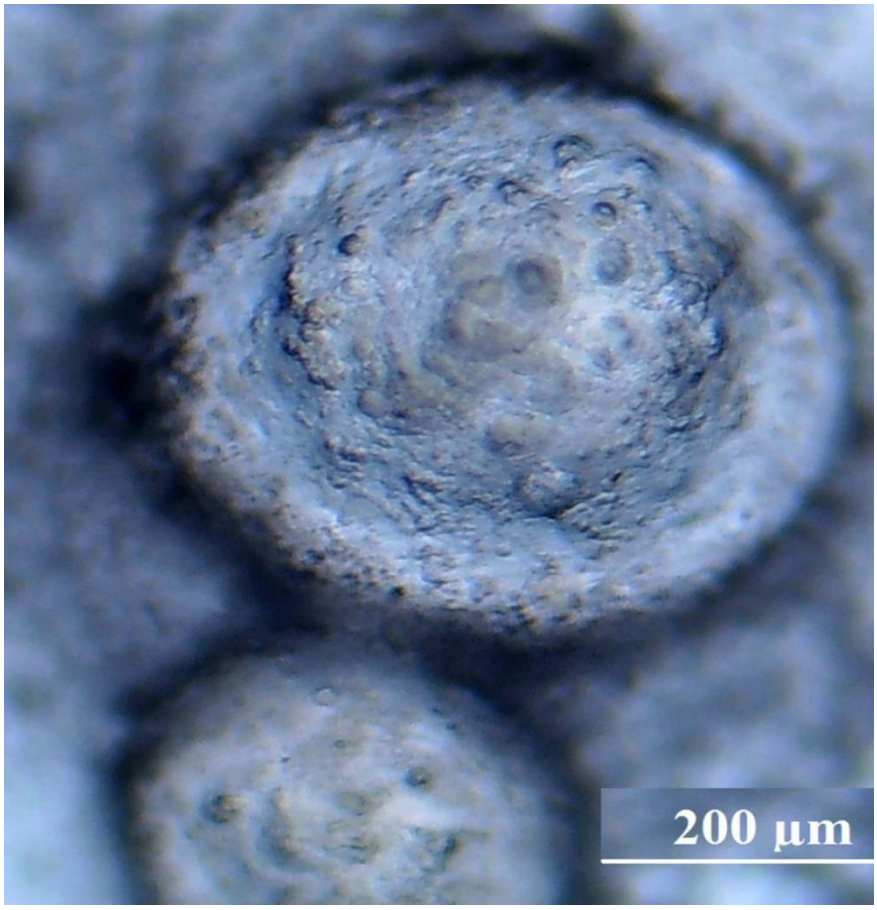

Figure 5.24 Electron microscopic image of CAP loadedAl^{3+}cross-linked buoyant IPN microbeads

5.4.3.1.2 Scanning Electron Microscopy (SEM)

The scanning electron microscopic image of the formed buoyant IPN microbeads showed porous and smooth spherical surface Figure 5.25. The appearance of pores was due to the generation of CO_2 as when basic $NaHCO_3$ reacted with acidic HCl an effervescent reaction occurred leaving CO_2 to liberate which released by penetrating the polymeric surface of the IPN microbeads [Choi et al., 2002].

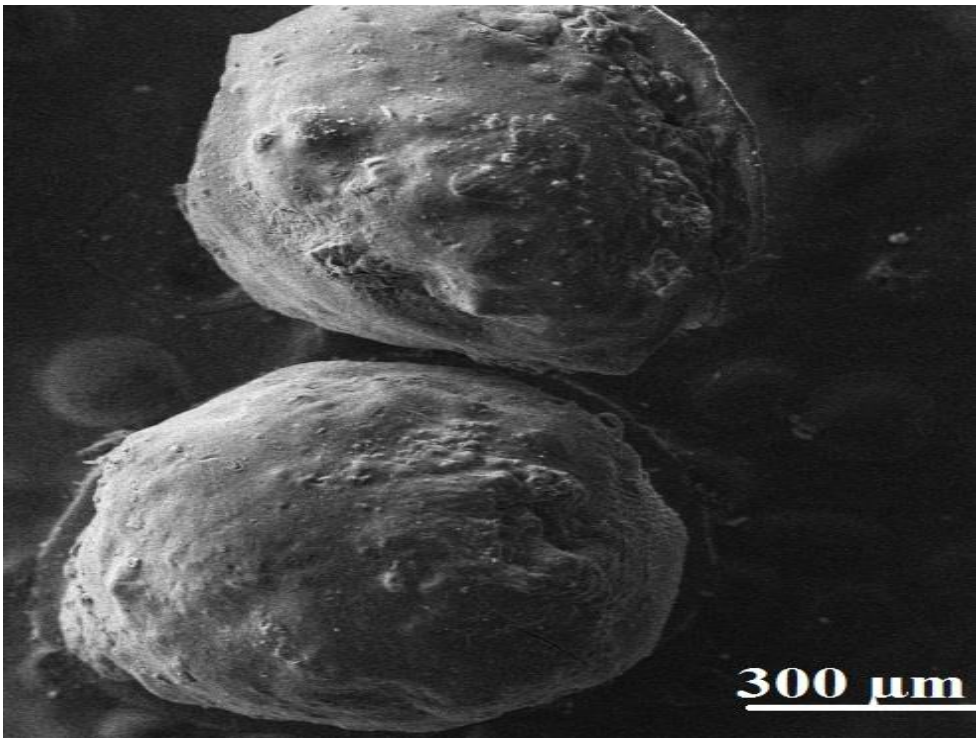

Figure 5.25 Scanning electron microscopic image of CAP loaded buoyant Al^{3+}cross-linked IPN microbeads

5.4.3.2 Energy Dispersive X-ray (EDX)

The study was proposed to determine the elemental framework and composition of buoyant aluminium ion cross-linked IPN microbeads. The analysis was done by EDX coupled with SEM and focussing the X-rays at a specific dense region of the sample as described earlier in **subsection 5.2.3.2** The results are shown in Figure 5.26 clearly depicts the presence of aluminium (Al=5.86%) and a trace quantity of sodium (Na= 0.6%) suggesting a successful

exchange of aluminium ion with sodium thus supporting cross-linking. The appearance of chlorine (Cl=11.8%) exhibits approximately complete adsorption of chlorine on the surface of microbeads. Presence of other elements such as carbon (C=27.04%) and oxygen (O=54.7%) also appeared during EDX analysis on the surface of microbeads.

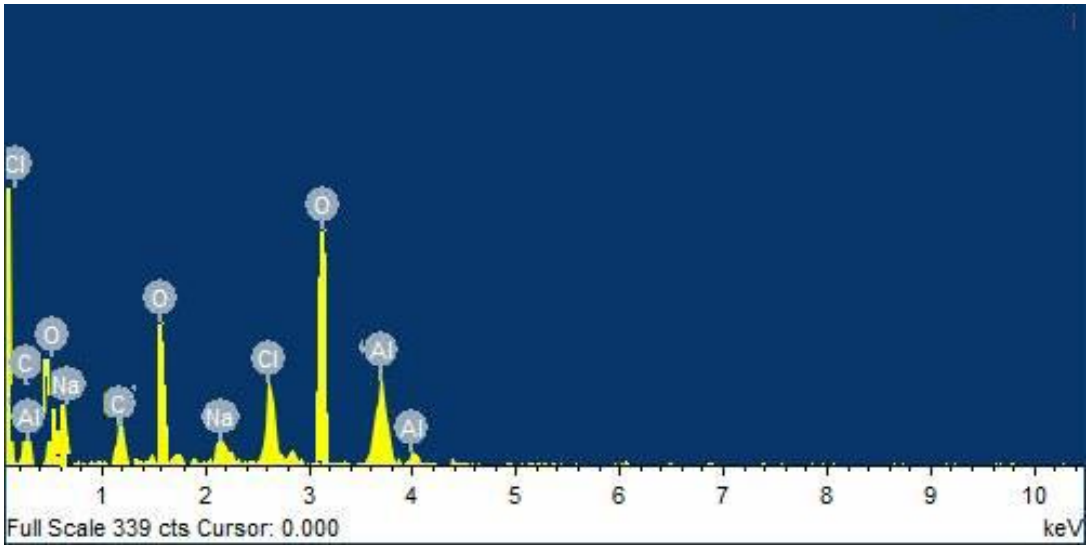

Figure 5.26 Elemental composition of the CAP loaded buoyant Al^{3+}cross-linked IPN microbeads

5.4.3.3 Fourier Transform Infra-Red spectroscopy (FTIR)

FTIR study was performed to investigate the possible drug-polymer interaction before and after the development of formulation [Adena et al., 2018]. The FTIR spectra of pure drug, LBG, NaAlg, physical mixture and all the optimized formulation F-1, F-2 and F-3 are presented in Figure 5.27. The LBG spectrum showed characteristic peaks at 3428 cm^{-1} due to O-H stretching, 2498 cm^{-1} due to C-H stretching, and 1780 cm^{-1} due to C=O stretching. NaAlg exhibited the distinctive peaks at 3493 cm^{-1} due to O-H stretching, 1618 cm^{-1} and 1417 cm^{-1} due to the asymmetric and symmetric stretching vibration of –COO functional groups respectively. The FTIR spectrum of pure drug CAP showed its characteristic absorption peaks at 3519 cm^{-1} due to O-H stretching, 3112 cm^{-1} due to N-H stretching, 1688

cm^{-1} due to pyrimidine carbonyl stretching vibration, 1041 cm^{-1} due to C-F stretching and 1206 cm^{-1} due to tetrahydrofuran ring. With respect to the physical mixture and all the optimized formulation (F-1, F-2 and F-3) all relevant peaks of drug and polymers were present without the appearance of any new peak suggesting all the components are compatible with each other.

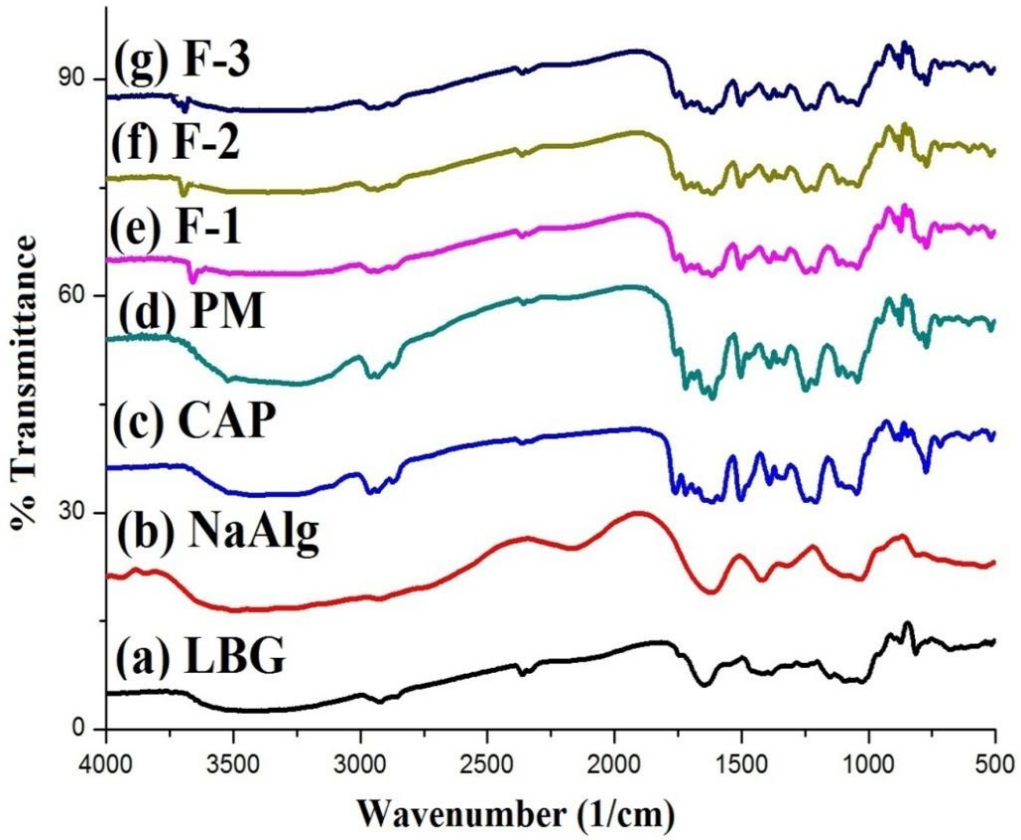

Figure 5.27 FTIR spectrum of (a) LBG, (b) NaAlg, (c) CAP, (d) PM, (e) F-1, (f) F-2, (g) F-3

However, the only point that was noticeable in all optimized formulation spectra was shifting of O-H stretching peak and –COO stretching peak towards higher wave number. The shifting of O-H peak indicated the formation of hydrogen bond between the polymers LBG and NaAlg and shifting of –COO functional group suggested the interaction of Ca^{2+} and Al^{3+} with carboxylic group of NaAlg. The interaction occurred due to the affinity of calcium and aluminum ion with sodium alginate. Both the hydrogen bonding and intercalation of metallic

ion are the utmost requirement for an IPN to be formed. Thus, the spectra of all the formulations clearly depict the successful development of IPN microbeads.

5.4.3.4 X-ray Diffraction (XRD)

XRD analysis was conducted to determine the crystalline nature of drug in its pure form and inside the polymeric matrix. The XRD spectra recorded for pure drug, LBG, NaAlg, physical mixture and optimized formulations (F-1, F-2, and F-3) are illustrated in Figure 5.28. The diffractogram obtained for pure drug CAP showed exhibited distinctive 2θ peaks at 10.05°, 10.08°, 10.55°, 10.64°, 10.68°, 15.6°, 17.88°, 18.7°, 20.45°, 21.83°, 22.89°, 24.72° and numerous minor peaks up to 30° suggesting the crystalline property of drug. The diffractograms of polymers LBG and NaAlg obtained showed peaks of small and diffused intensity and broad halo peaks. The XRD spectrum of physical mixture exhibited nearly all the peaks of drug and polymers without any physical change. However, the XRD pattern of all the optimized formulation showed peaks of abridged intensity indicating that pure drug has now converted into amorphous form on getting entrapped within the polymeric matrix [Upadhyay et al., 2018b].

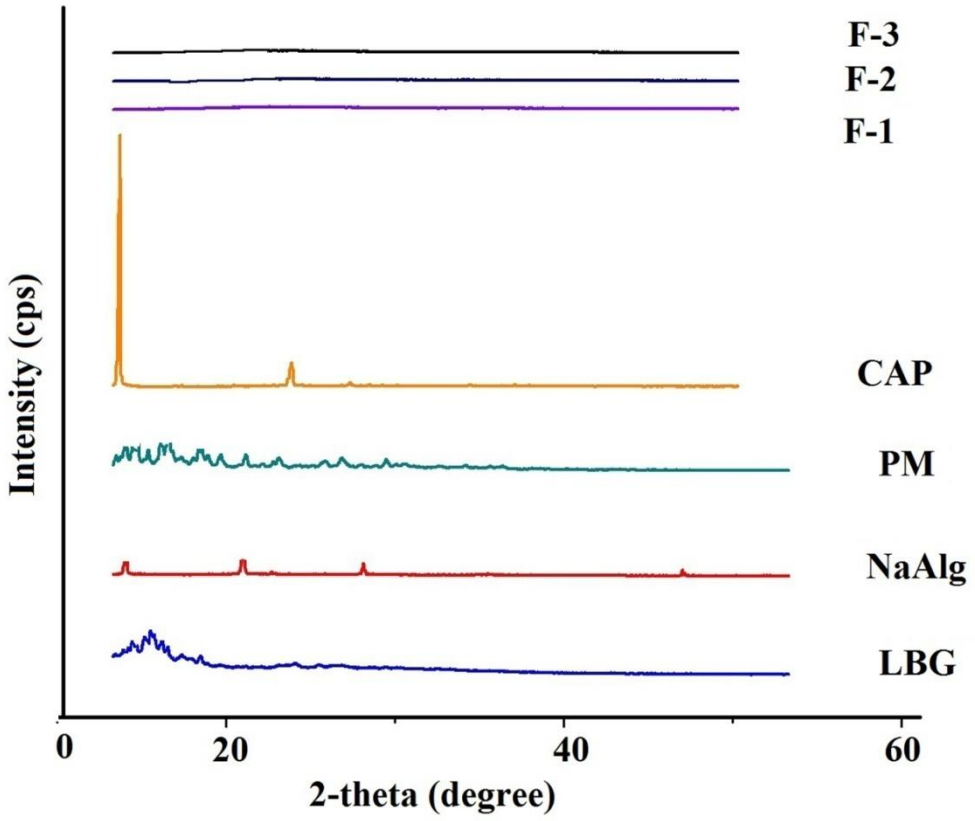

Figure 5.28 XRD spectra of polymers (LBG and NaAlg), Physical mixture (PM), pure drug (Capecitabine; CAP) and optimized formulations (F-1, F-2 and F-3)

5.4.3.5 Differential scanning calorimetry (DSC)

To understand response of drug and its formulation towards thermal stress is a necessary requirement during the development of a stable medicinal product. DSC is the most preferred thermal analytical technique that givesdetailed information ofphysical and energetic property of the substances[Clas et al., 1999]. The DSC thermograms recorded for drug, LBG, NaAlg, and optimized formulations (F-1, F-2 and F-3) are exhibited in Figure 5.29. The polymers LBG and NaAlgdisplayed their distinctive melting peaks at 90.53°C and 186.16°C. The pure drug CAP showed two sharp peaks at 123.76°C corresponding to its melting peak and another peak at156.80°C due to thermal decomposition [Agnihotri and Aminabhavi, 2006]. In case of optimized formulation, the thermograms appeared were flat and without any

melting and decomposition peak that was present in the pure drug. Thus, revealing the successful conversion of crystalline pure drug into an amorphous form.

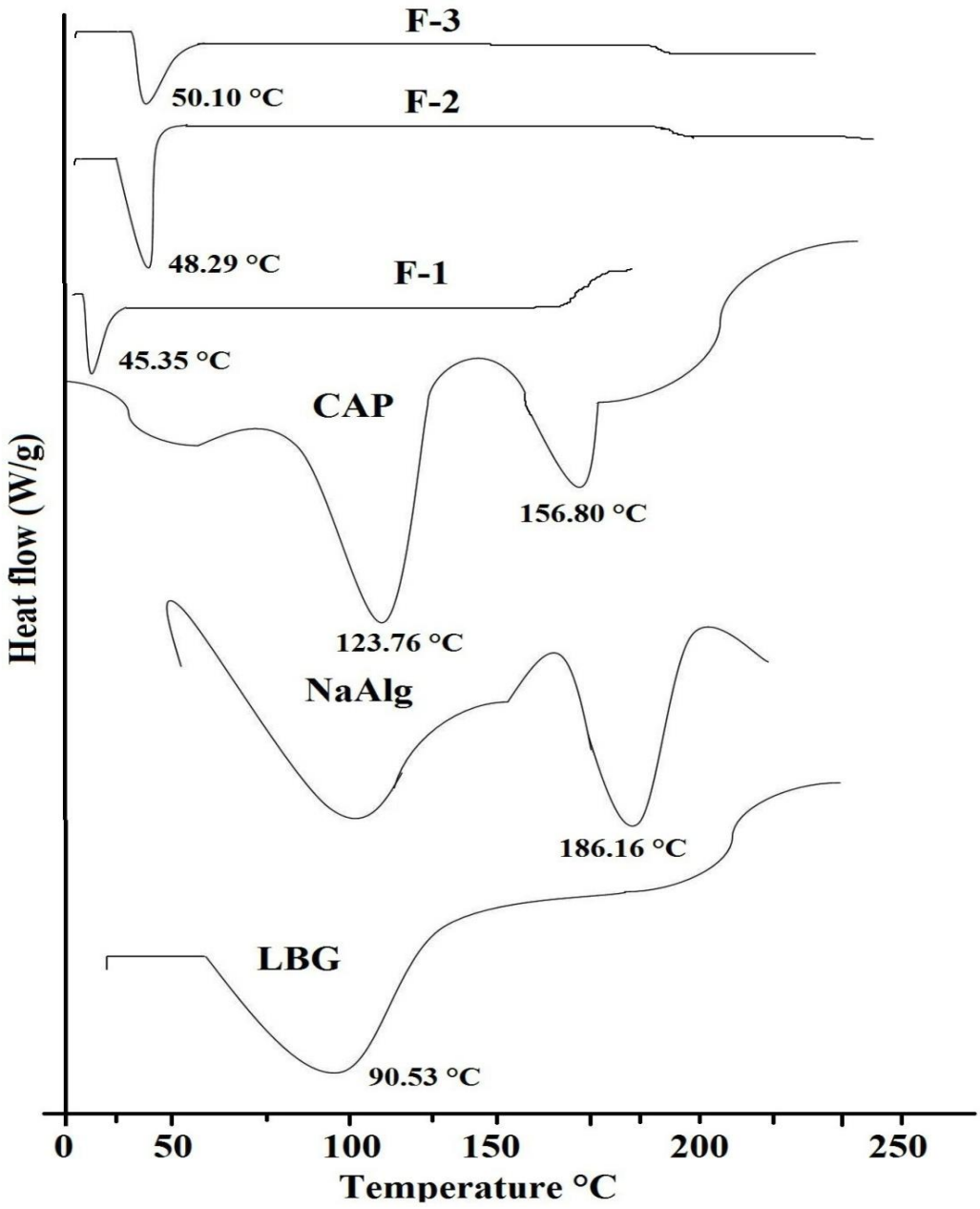

Figure 5.29 DSC Thermograms of LBG, NaAlg, CAP, F-1, F-2 and F-3.

5.4.3.6 Drug entrapment (%)

The drug entrapment efficiency of CAP loaded buoyant IPN microbeads was ranged from 57.85 ± 1.6% to 94.69 ± 2.34% (Table 5.11). It was observed that drug entrapment was increased with increase in the ratio of LBG: NaAlg and the concentration of cross-linker. Increase in the drug entrapment with an increase in the ratio of LBG:NaAlg was due to the more viscous and less hydrophilic nature of LBG. The property of solubility in polysaccharides is governed by mannose component whose value is reported as 4 in comparison to NaAlg which is 1[Picout et al., 2002]. Thus, LBG showed limited solubility and maximum volume expansion thus; hold the drug firmly in the polymeric blend of LBG and NaAlg. Another factor that promoted the drug entrapment was the concentration of cross-linker. More the cross-linker more the intricated network was formed within the polymeric matrix. As the cross-linker used was a trivalent Al^{3+}, so it bound with three guluronicunits of NaAlg and associates firmly thus prevent the leaching of drug into the external media.

5.4.3.7*In vitro* buoyancy study

The result of *in vitro* % buoyancy, floating lag time (FLT) and total floating time (TFT) is shown in Table 5.14. The floating behaviour of trivalent ion cross-linked IPN microbeads is also shown in Figure 5.30. The buoyancy of the microbeads can directly be related with the bead density and amount of sodium bicarbonate ($NaHCO_3$). Both the components played a permissive role in influencing the buoyancy [Bera et al., 2015]. The formulations with higher content of LBG (with respect to viscosity) showed more bead size with high density and retained higher amount of water in the matrices that lead to an increase in the weight of the microbeads thus less number of microbeadsappeared on the surfaceresulting lower % buoyancy and greater onset of time to reach on the surface of the media[Carbinatto et al., 2014]. Another factor $NaHCO_3$ enhanced the floating time of the formed IPN microbeads.

This can be explained as when $NaHCO_3$ came in contact with acidic media (pH 1.2 0.1 N HCl) it liberated carbon dioxide (CO_2) and the generated gas got entrapped within the polymeric gel layer between LBG and NaAlg thus decreased the density of the IPN microbeads and the beads became buoyant[Li et al., 2014].The mean density of all the batches was found to be less than that of SGF i.e. less than 1.004 g/cm^3. The FLT of the batches varied from 2:10 ± 0.19 min to 5:30± 0.38 min. The variation observed was based on the density of the formulation in the batches. The TFT of formulations in an average was found to be approximately > 10 h.

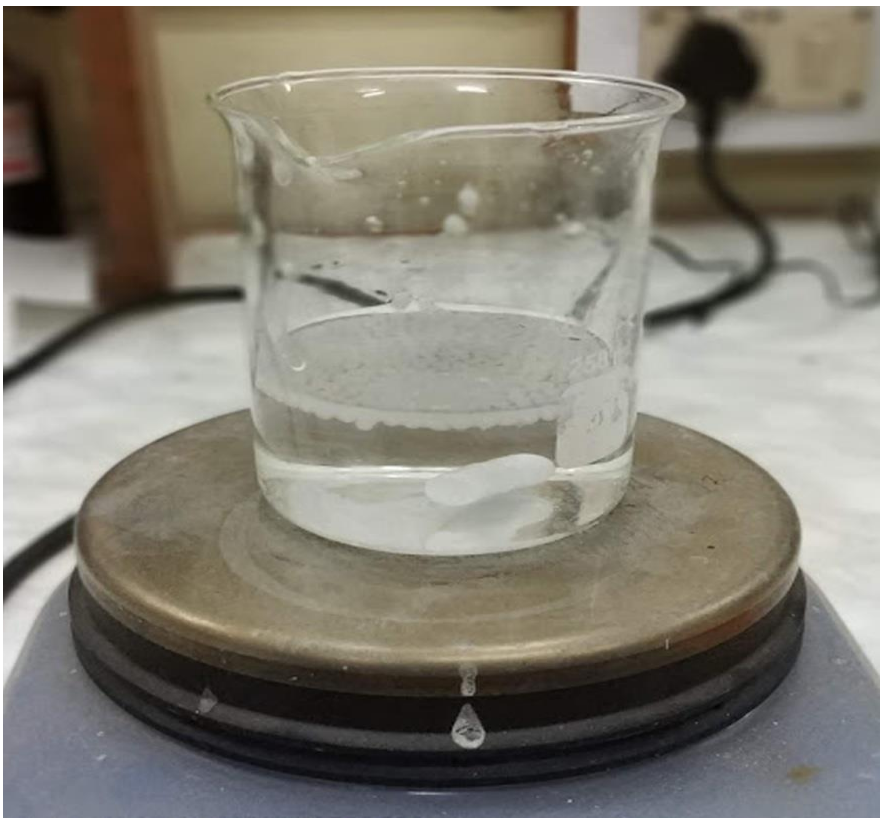

Figure 5.30 Prepared buoyant IPN microbeads

Table 5.14 Estimated density, diameter, floating lag time (FLT) and total floating time (TFT) of formed buoyant IPN microbeads

Batch	[a]Diameter (mm^3)	[a]Density (g/cm^3)	FLT (min)	TFT (h)
1	1.57±0.03	0.79±0.08	4.45±0.22	10
2	1.36±0.09	0.47±0.1	2:15±0.32	>10
3	1.49±0.04	0.72±0.06	4:35±0.70	>8
4	1.42±0.01	0.69±0.02	3:20±0.43	>12
5	1.33±0.11	0.50±0.01	2:18±0.23	>8
6	1.92±0.07	0.95±0.06	5:40±0.18	>10
7	1.39±0.09	0.55±0.05	3:07±0.45	>10
8	1.47±0.05	0.66±0.03	3:15±55	>10
9	1.70±0.07	0.92±0.02	5:30±0.21	8
10	1.52±0.02	0.76±0.04	4:40±0.20	>8
11	1.60±0.12	0.82±0.03	5:10±0.64	>8
12	1.65±0.07	0.88±0.09	5:18±0.40	10
13	1.35±0.05	0.44±0.09	2:10±0.27	>10
14	1.85±0.03	0.90±0.02	5:28±0.36	8
15	1.44±0.02	0.61±0.08	3:10±0.33	>10

[a]Mean ± SD; n=3

5.4.3.8 Swelling study

Swelling study of the formulation was performed to study the transport of water molecules inside the microbeads (Table 5.7) [Agnihotri and Aminabhavi, 2006]. The study of all formulations were conducted in simulated gastric fluid pH 1.2 and simulated intestinal fluid (SIF) pH 6.8 as a function of time. Swelling profile of all types of IPN microbeads i.e. calcium ion cross-linked, aluminum ion and aluminum ion cross-linked buoyant IPN microbeads are displayed in Tables 5.15, 5.16 and 5.17 respectively. It was found that the formulations having more LBG showed more swelling. Since NaAlg hydrates and dissolves easily when comes in contact with water whereas LBG retains the water molecules and increases in size leading to the expansion of polymer matrix thus, showed good swelling index values [Prajapati et al., 2015]. On the other hand, degree of cross-linking also affected swelling. More the cross-linker lesser the swelling happened due to lack of free

hydrodynamic value[Kaity et al., 2013a]. A brief description of factors that affected swelling are described as follows:

(a) Polymeric ratio

Both polymers were responsible for swelling of the microbeads however LBG exhibited important role in comparison to NaALg. LBG and NaAlg both are polysaccharides comprised of galactomannan units where mannose (M) and galactose (G) shows hydrophobic and hydrophilic nature, respectively. In case of LBG the ratio of M/ G is 4:1 due to this reason it showed limited solubility and more viscous nature in comparison to NaAlg which got hydrated by forming hydrogen bond in water. Hence, the polymeric blend of LBG and NaAlg exhibited higher swelling in presence of high amount of LBG [Pollard et al., 2008].

(b) Effect of Cross-linker

The cross-linkers, bivalent and trivalent ions calcium (Ca^{2+}) and aluminum (Al^{3+}) ions respectively exhibited an important effect on swelling. It was found that with an increase in the concentration of both the cross-linkers lead to the formation of rigid matrix causing a reduction in the pore volume of the IPN matrix hence, reduction in the size of the beads appeared [Bhattacharya et al., 2012].

(c) Effect of pH

Swelling index values of the formed IPN beads was found to be different in different pH media i.e. pH 1.2 and pH 6.8. At low pH (pH 1.2) the carboxyl group present in the polymers undergoes protonation and lead to the formation of strong

formation of strong hydrogen bond, thus, reduction in the swelling index value. However, at high pH (pH 6.8) process of deprotonation occurs leading to the strong electrostatic repulsion force between the ionized acidic functional groups thus, swelling value was increased [Leong et al., 2011].

Table 5.15 Estimated swelling index of calcium ion cross-linked formed IPN microbeads

Batch no	LBG:NaAlg (% w/v)	Cross-linker (% w/v)	Swelling index[a] (%)	
			pH 1.2	pH 6.8
1	3:1	2	467.12 ± 1.3	665.42 ± 2.70
2	1:3	3	252.92 ± 4.3	555.42 ± 1.34
3	1:1	2	393.29 ± 3.7	589.46 ± 1.90
4	1:1	4	359.27 ± 1.1	565.82 ± 4.70
5	1:1	2	390.54 ± 2.6	592.44 ± 2.80
6	3:1	3	459.29 ± 3.7	650.89 ± 3.20
7	1:1	3	355.45 ± 2.19	572.71 ± 1.85
8	3:1	3	459.29 ± 1.75	650.89 ± 1.1
9	1:1	3	370.33 ± 3.23	575.22 ± 3.65
10	1:3	2	261.61 ± 1.96	562.34 ± 2.75
11	3:1	4	449.18 ± 2.77	660.29 ± 2.55
12	1:3	3	255.11 ± 1.76	545.11 ± 3.89
13	1:3	4	240.70 ± 3.77	530.69 ± 2.04
14	1:1	3	372.19 ± 1.87	570.51 ± 3.1
15	1:1	4	362.25 ± 2.55	560.19 ± 2.91

[a]Mean± S.D.; n=3

Table 5.16 Estimated swelling index of aluminum ion cross-linked formed IPN microbeads

Batch No	LBG:NaAlg (% w/v)	Cross-linker (% w/v)	Swelling index[a] (%)	
			pH 1.2	pH 6.8
1	1:3	2	253.23 ± 3.8	549.71± 2.33
2	1:3	3	245.31 ± 1.34	537.11 ± 2.89
3	3:1	3	451.29 ± 2.56	648.54 ± 2.77
4	3:1	3	448.60 ± 3.65	645.42 ± 3.80
5	1:1	3	247.36 ± 1.29	561.38 ± 2.14
6	1:3	3	241.64 ± 2.29	539.29 ± 2.76
7	1:3	4	227.91 ± 1.37	515.28 ± 1.49
8	3:1	2	456.51 ± 2.62	657.66 ± 3.76
9	1:1	2	379.40 ± 2.41	579.21 ± 3.70
10	1:1	2	375.43 ± 2.44	576.31 ± 1.50
11	1:1	3	367.74 ± 3.61	567.61 ± 3.22
12	1:1	4	351.22 ± 2.89	544.19 ± 2.55
13	3:1	4	434.39 ± 3.67	623.20 ± 3.02
14	1:1	3	361.59 ± 3.33	564.41 ± 3.72
15	1:1	4	347.33 ± 2.54	542.52 ± 3.44

[a]Mean± S.D.; n=3

Table 5.17Estimated swelling index of aluminum ion cross-linked buyoyantIPN microbeads

Batch No	LBG:NaAlg (% w/v)	Cross-linker (% w/v)	Swelling index[a] (%)	
			pH 1.2	pH 6.8
1	1:1	2	382.22 ± 4.8	585.19 ± 1.9
2	1:3	3	247.16 ± 3.4	540.27 ±1.9
3	1:1	3	250.40 ±4.1	560.32 ± 5.3
4	1:1	4	349.86 ±2.8	550.18 ± 1.4
5	1:3	4	230.89 ± 4.1	512.18 ±3.3
6	3:1	2	452.54 ± 2.1	652.88 ±3.5
7	1:3	2	257.06 ±2.5	547.35 ±4.4
8	1:1	3	248.11 ±4.3	560.24 ±4.7
9	3:1	3	449.48 ±1.7	649.49 ± 5.4
10	1:1	2	380.41 ± 4.9	581.29 ±2.7
11	3:1	4	430.13 ± 3.9	620.18 ± 2.6
12	3:1	3	450.52 ±1.1	646.91 ±1.9
13	1:3	3	249.54 ± 3.3	537.08 ± 2.6
14	3:1	3	446.33 ± 3.7	642.86 ± 2.2
15	1:1	4	352.28 ± 3.5	550.61 ± 1.9

[a]Mean± S.D.; n=3

5.4.3.9 *Ex vivo* mucoadhesion

The result of wash off test performed to evaluate the mucoadhesion of the microbeadsin two different test fluids is exhibited in Table 5.18. The percentage of microbeads adhered to the mucosal tissueingastric fluid at pH 1.2 was found in the range of 86 ± 3.43% to 38 ± 1.22% and 34 ± 1.01% to 02 ± 2.1% at pH 6.8. The relative rapid wash off at high pH than at low pH may be attributed to the degree of protonation at different pH condition. Bio adhesive polymers that are used in controlled drug delivery applications generally possess polyanions commonly carboxyl and hydroxyl functional group[Rahamatullah Shaikh et al., 2011]. These functional group at low pH undergoes protonation where they attach to the mucous membrane by several interactions such asan ionic bond, hydrogen bond and Van der Waal's forces [Pliszczak et al., 2012]. All these interactions especiallyhydrogen bond actively maintains and hold the formulation with the glycosylated protein mucin present in the

epithelial tissues in animals[Park and Robinson, 1985]. Another factor that affected the rapid wash off of the microbeads at high pH might be due to the presence of excessive moisture pH 6.8 resulted into a slippy mucilage surface that was not able to retain the microbeads for a longer time relativeto low pH [McCarron et al., 2004].

Table 5.18 % Mucoadhesion of the formed buoyant IPN microbeadsin two different pH 1.2 & pH 6.8

Batch No	LBG:NaAlg (% w/v)	Cross-linker (% w/v)	Mucoadhesion[a] (%)	
			pH 1.2	pH 6.8
1	1:1	2	70 ± 3.8	10 ± 2.5
2	1:3	3	40 ± 4.2	06 ± 4.4
3	1:1	3	49 ± 1.9	09 ± 4.9
4	1:1	4	58 ± 2.4	08 ± 5.7
5	1:3	4	38 ± 4.4	02 ± 2.0
6	3:1	2	86 ± 1.3	34 ± 1.9
7	1:3	2	54 ± 1.8	06 ± 2.6
8	1:1	3	42 ± 3.907	±5.5
9	3:1	3	80 ± 2.829	±1.8
10	1:1	2	65 ± 3.1	07 ± 1.8
11	3:1	4	75 ± 3.9	14 ±1.9
12	3:1	3	82 ± 4.2	32 ± 2.8
13	1:3	3	44 ± 2.9	04 ± 3.1
14	3:1	3	78 ± 2.425	±5.5
15	1:1	4	61 ±1.308	± 1.8

[a]Mean± S.D.; n=3

5.4.3.10*In vitro* drug release study

In vitro drug release of the optimized buoyant trivalent ion cross-linked microbeads was carried out in 900 mLof 0.1 N HCl (pH 1.2) for 8 h followed by in 900 mL of phosphate buffer (pH 6.8) for remaining 20 h in USP type II dissolution apparatus. The optimized microbeads showed 10% drug release for the first 2 h and 44% drug release for remaining 6 h followed by the extended release of drug from polymeric matrix for the next 12h at pH 6.8 (Figure 5.31). Drug release from the hydrophilic polymeric matrix is considered as a

combined phenomenon of swelling and diffusion[Shakya et al., 2013]. At pH 1.2 a constant sustained release of CAP was observed from the buoyant IPN microbeads till 8 h may be due to the combined effect of swelling, diffusion and presence of pores in the microbeads. LBG is a highly viscous and low water soluble biopolymer in comparison to NaAlg[Dionísio and Grenha, 2012b]. When the microbeads were placed in simulated gastric fluid (SGF), due toprotonation less swellingoccurred resulted in the slow drug release however presence of pores allowed multiple entries for the media to enter inside the matrix that resulted into maximum but slowdiffusion of drug from the polymeric matrix till 8 h. Further, at pH 6.8 extended and maximum i.e. 50% drug release was observed due to change in pH lead to the deprotonation resulted into more swelling and more ions in the buffer media increases, leading to the increase in the osmotic force and electrostatic force that resulted into continuous notable extended release which directly loosen the polymer network thus, more release was observed.Apart from diffusion and pore formation in the cross-linked IPN microbeads, another factor that played an additive effect in extending the release till 20 h was the pure drug CAP inherent property. With respect to CAP, it is already reported that an amorphous CAP possesses low glass transition temperature thus turns into a gel that might also slow down the drug release from the formulation [Meulenaar et al., 2013]. The kinetic data observed for the above formulation showed a maximum R^2 value of 0.991 in case of zero order release kinetics.

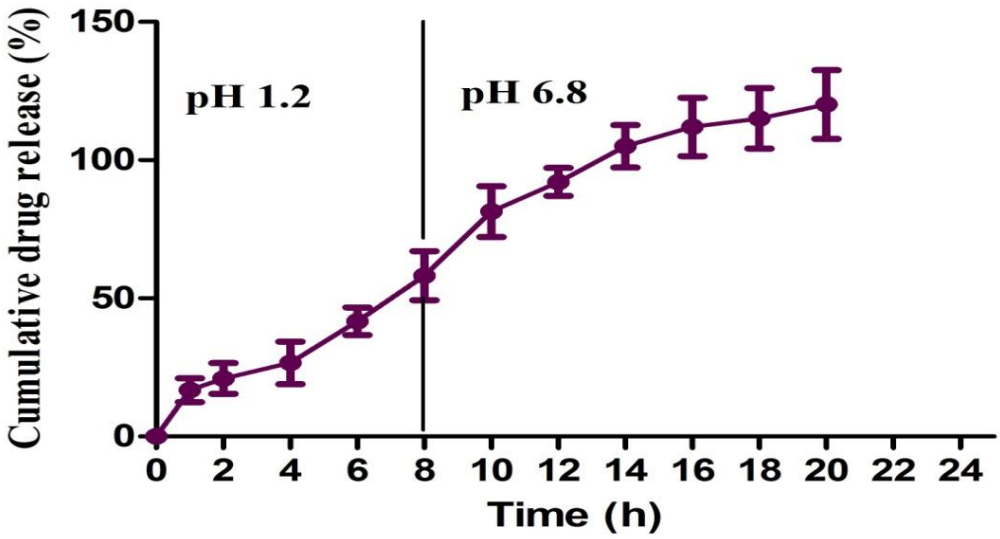

Figure 5.31 *In vitro* Drug release profile of optimized buoyant cross-linked IPN microbeads (vertical bars represent mean± S.D. n=3)

5.4.3.11*In vitro* cell cytotoxicity study

Cell cytotoxicity study was performed on adherent type human colon cancer HT-29 cell lines by sulforhodamine B assay to analyse the percentage cell viability reduction caused by the optimized formulations (F-1, F-2 and F-3) in comparison to the pure drug (CAP), control (non-treated) and standard (Adriamycin®) [Vardhan et al., 2017]. The sample preparation for all the formulations was done in the varying concentration of 10-80 µg/mL. The result of the assay was interpreted in terms of GI_{50} defined as 50% cell growth inhibition [Chaurasia et al., 2015]. Figure 5.32 represents the images of comparative cell viability reduction for all the groups and standard. Figure 5.33 represents a graphical study profile plotted between % control growth and concentration revealing the maximum % growth inhibition caused at the minimum concentration of 10 µg/mL in case of all formulations. The images of the SRB assay clearly depicts that a maximum number of cell inhibition was observed in case ofstandard (Adriamycin®) and optimized formulations i.e. F1, F2 and F3 in comparison to free drug.

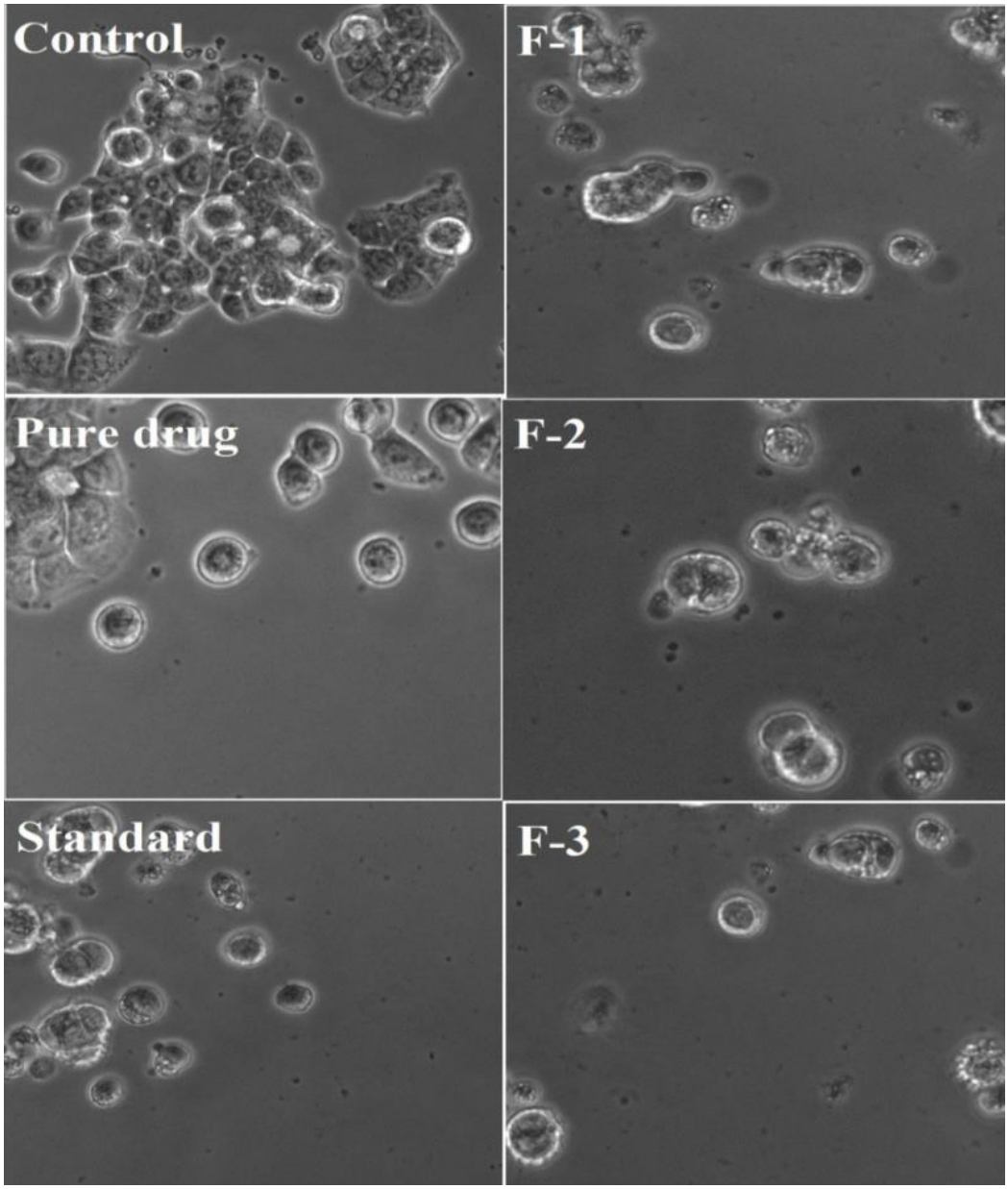

Figure 5.32 Comparative results of in vitro cytotoxicity study of optimized formulations against control, pure drug and standard

Polysaccharides possess the potential to cause immunomodulator and antitumor effect. CAP an anticancer when entrapped within polysaccharide matrix of LBG and NaAlgshowed good inhibition of cancer cell growth [c Ooi and Liu, 2000]. Both the polymers are reported active against several tumors[Eun Ju Cho and Rhee, 2006], specially LBG, that is rich in Gallic acid, an important phytochemical constituent, showed effective antiproliferative activity against HT-29 colon cancer cell line by inhibiting the DNA synthesis [Klenow et al., 2008].

The control group showed 100% cell growth as provided no treatment whereas the GI_{50}caused by optimized formulations showed higher cytotoxic action i.e.2.05 folds (F-1), 2.08 folds (F-2) and 2.09 folds in comparison to pure drug that was found to be 1.22 folds. Thus from the graph and the images it can be concluded that the formed optimized formulations are capable of inhibiting colon cancer cell growth.

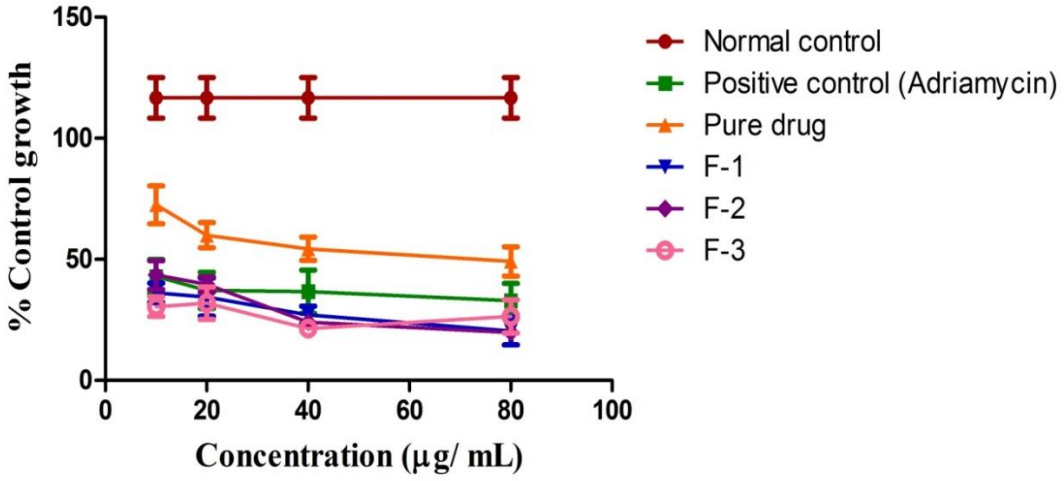

Figure 5.33Comparative graphical profile of SRB study plotted between % control growth and concentration (µg/mL) for different groups positive control, pure drug, and optimized formulation (F-1, F-2, and F-3)(vertical bars represent SEM n=3; p< 0.001 compared to pure drug; Two-way ANOVA: Bonferronipost test)

5.4.3.12Acute oral toxicity and histopathology

The acute oral toxicity performed exhibited no death during supervision period of 14 days after oral administration of optimized formulations F-1, F-2 and F-3. The oral dosing of 2000 mg/Kg, given to rats followed guidelines of OECD for the 'test of chemicals 425' adopted on 17th December2001 Annexure- 4. The objective of the test was to examine the effect of a lethal dose on mortality with the starting dose level of 2000 mg/Kg. Results indicated that the test product can be classified as "Category 5" with "zero" toxicity.

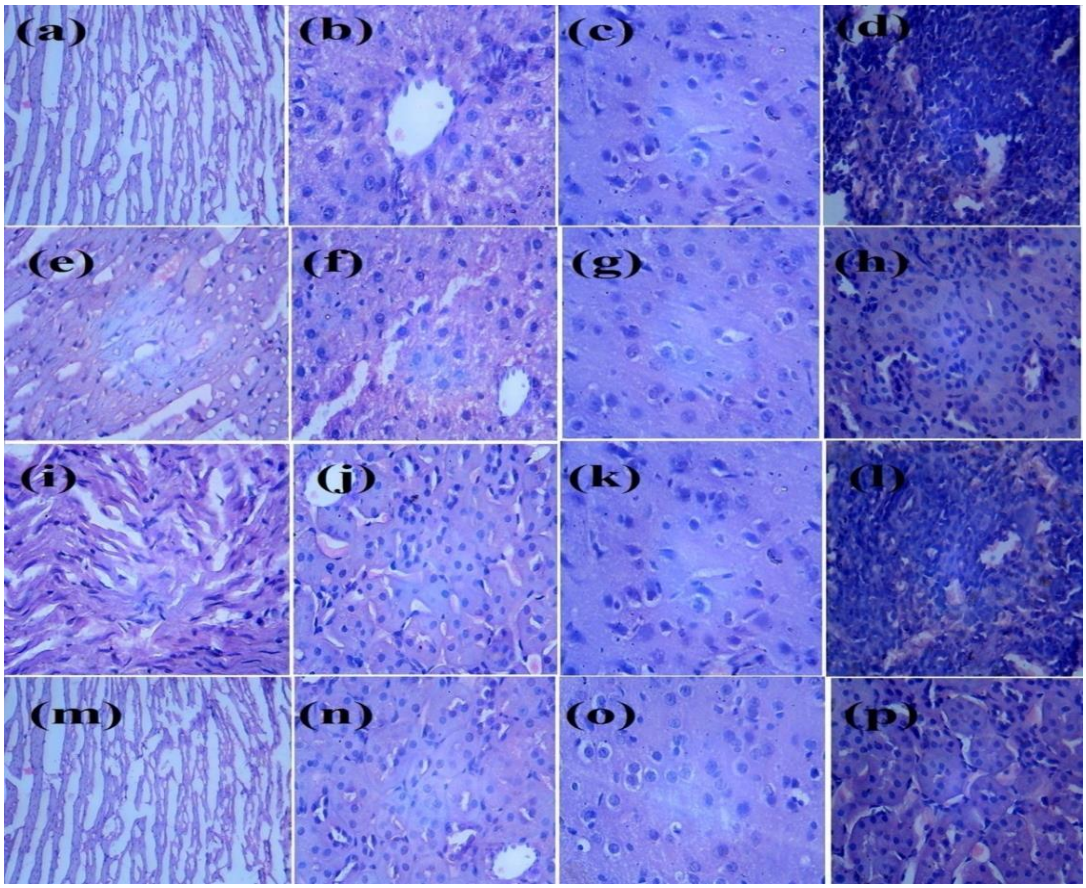

Figure 5.34 Microscopic images of histopathological sections of major organs of normal control (a) heart (b) liver (c) kidney (d) spleen; F-1 (e) heart (f) liver (g) kidney (h) spleen; F-2 (i) heart (j) liver (k) kidney (l) spleen; F-3 (m) heart (n) liver (o) kidney (p) spleen

Further, the images of harvested major organs sectioned during histopathology study for the groups, normal control and optimized formulations F-1, F-2 and F-3 presented in Figure 5.34 showed similarity with each other with respect to presenceof major organs such as, heart of normal control showed cardiac myocytewith centrally located nucleus, perkinje fibre and intercalated disc (Figure 5.34a). Similar morphology was observed in the case of formulation group (Figure 5.34e,i, m for F-1; F-2; and F-3, respectively). Another micrographic image of the liver of both, control (Figure 5.34b) and formulations group (Figure 5.34f,j,n for F-1, F-2 and F-3, respectively) exhibited polygonal cells with central nuclei and Kuppfer cells. Histopathology of kidney showed cuboidal epithelial cells of the loop of Henle in control

group (Figure 5.34c) and in formulation group (Figure 5.34g,k,o for F-1, F-2 and F-3, respectively). In case of histology of spleen presence of pulps i.e. white pulp and red pulp in control group (Figure 5.34d) and formulation group (Figure 5.34h,l,p for F-1, F-2 and F-3 respectively) showed indifference with each other thus, it was found that no morphological changes or lesions appeared in all the groups indicating that IPN microbeads of CAP are safe for oral administration without any toxic manifestation.

5.4.3.13 Stability study

The stability study performed for the optimized batch of the buoyant IPN microbeads stored at three different conditions i.e. refrigeration temperature (5°C ± 3 °C), room temperature (25°C ± 2°C with 70 ± 5% RH), and at high temperature (40°C ± 2 °C with 75 ± 5% RH) exhibited non- significant ($p>0.05$) differences for the physical attributes particle size, % drug entrapment and % total drug content in comparison to the fresh prepared sample of the same batch (Table 5.19). The obtained shelf-life of the batch was 19.8 months, 19.4 months and 9.5 months respectively (Figure 5.35).

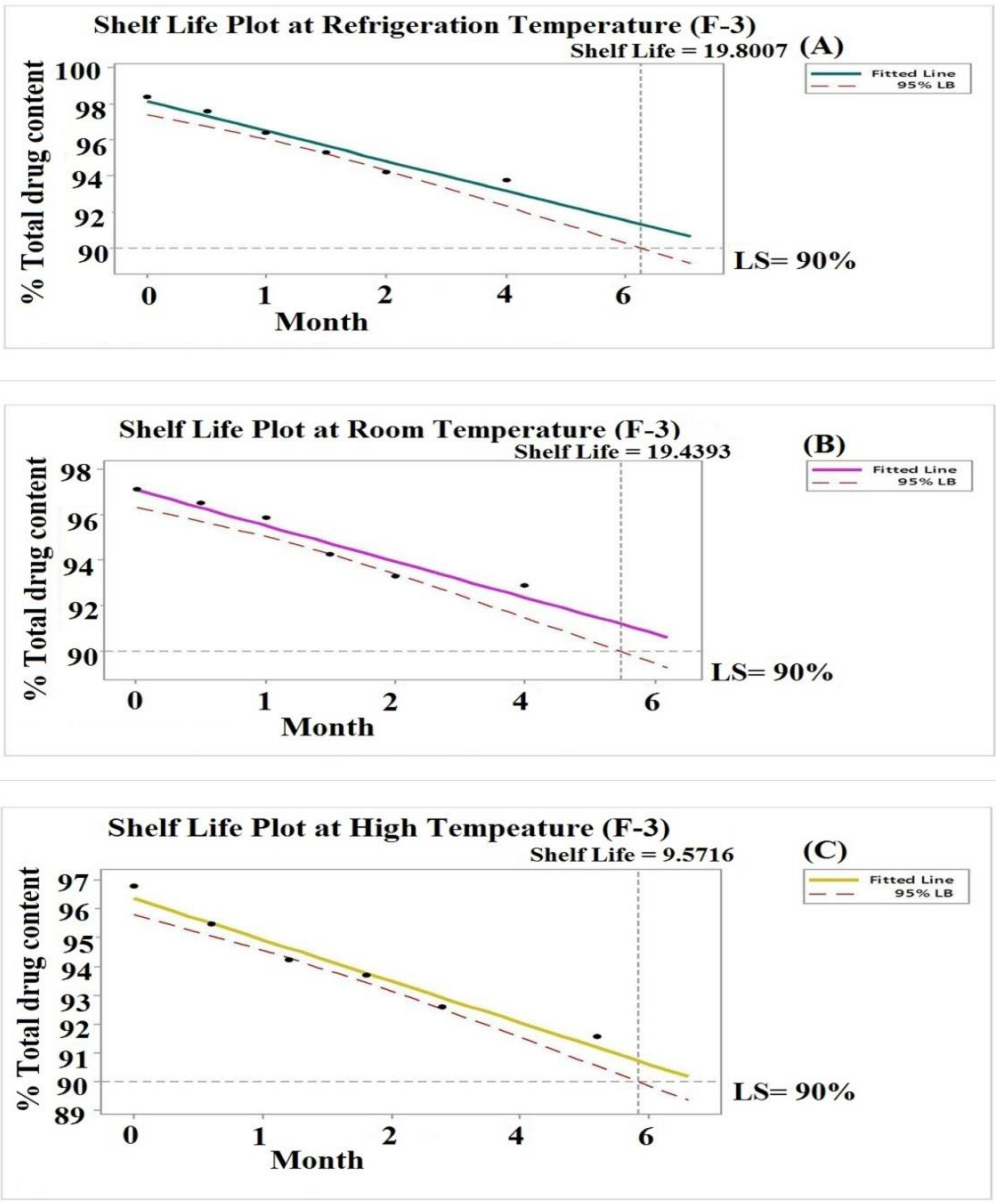

Figure 5.35 Shelf-life plots of the optimized batch of cross-linked buoyant IPN microbeads stored at (A) refrigeration temperature, (B) room temperature and (C) high temperature with low specification (LS) at 90%.

The results of storage temperature at refrigeration and at room temperature were almost in the close vicinity indicating the formulation to be stable at both temperatures. And also in all cases, the shelf-life of the formulations at refrigeration temperature was found to be highest suggesting it to be safe and stable for long term use when kept at a cool place.

Table 5.19Results of stability study of trivalent ion cross-linked buoyant IPN microbeads stored for 6 months

At the end of 6 months				
Parameters	**[a]Fresh prepared sample**	**[a]Refrigeration Temperature**	**[a]Room Temperature**	**[a]High Temperature**
Particle size (µm)	405.16 ± 1.7	404. 96 ± 2.1	402.92 ± 1.8	400.32 ± 1.9
Drug entrapment (%)	83.67 ± 2.9	82.79 ± 1.7	80.89 ± 2.7	79.66 ± 1.8
Total drug content (%)	99.72 ± 1.1	98.39 ± 2.7	97.11 ± 2.8	96.78 ± 2.1

[a]Mean± S.D.; n=3**.**

5.4.3.14 *In vivo* pharmacokinetic study

Figure 5.36 and Table 5.20 summarizes the results of*in vivo* pharmacokinetic study. *In vivo* study of the optimized formulations (F-1, F-2 and F-3) showed promising results in comparison to the pure drug in solution form. At all-time points a high and notable significant difference was observed between optimized formulations (F-1, F-2, and F-3) and pure drug (CAP) in solution form. The AUC of optimized formulation F-1 (5.04 ± 0.34 µg-h/mL); F-2 (9.38 ± 0.31 µg-h/mL) and F-3 (17.23 ± 0.29 µg-h/mL) was increased 1.85 folds, 3.456 folds and 6.346 folds respectively. MRT of the optimized formulations F-1 (6.694 ± 0.85 h), F-2 (11.591 ± 0.90 h) and F-3 (20.177 ± 0.94 h) increased 3.45 folds, 5.974 folds and 10.40 folds respectively. Both parameters AUC and MRT indicated better bioavailability of CAP from IPN microbeads in comparison to the pure drug. Further, the lower C_{max} value of all three formulations in comparison to pure drug might be due to slow absorption of CAP from IPN microbeads. An increased $t_{1/2}$ were also observed in case of all the formulations such as 7.87 folds (4.388 ± 2.71 h) for F-1, 12.53 folds (6.98 ± 2.85 h) for F-2 and 24.044 folds for F-3 (13.39 ± 2.88 h) when compared to pure drug that showed $t_{1/2}$ of 0.55 ± 0.12 h revealing the

slower elimination and longer half-life by the formulation. Thus; the overall data of the pharmacokinetic study illustrates that all the formulations showed a significant and detectable content of CAP from the IPN microbeads formulations into systemic circulation for 12 h. However, among all the three formulations F-3 showed enhanced AUC, MRT and $t_{1/2}$ values that may be due to the gastro retention property imposed by it due to its increased residence time in GIT.

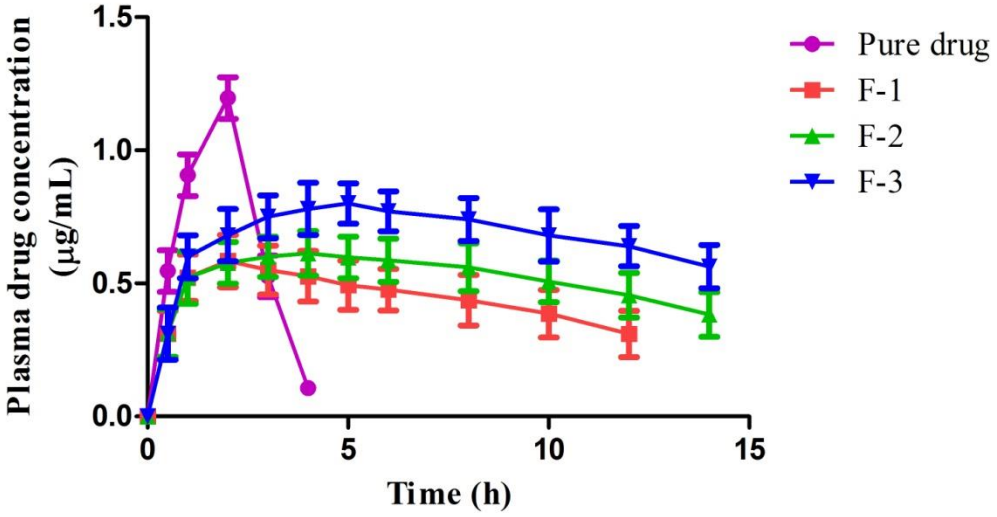

Figure 5.36 Comparative in vivo plasma drug concentration-time profiles of pure drug and optimized formulations (F-1, F-2 and F-3) following oral administration in rats. (Vertical bars represent SEM; n=6)

Table 5.20 Calculated PK parameters of pure drug (Capecitabine) and optimized formulation (F-1, F-2 and F-3)

PK Parameters	**[a]Pure drug**	**[a]F-1**	**[a]F-2**	**[a]F-3**
C_{max} (µg/mL)	1.2 ± 0.25	0.59 ± 0.14	0.61 ± 0.16	0.90 ± 0.19
T_{max}(h)	2.0 ±0.0	2.0 ± 0.0	4.0 ± 0.0	5.5 ± 0.0
$AUC_{(0-t)}$ (µg-h/mL)	2.715 ± 0.435	5.040 ± 0.34	9.38 ± 0.31	17.23 ±0.29
MRT (h)	1.940 ±0.61	6.694 ± 0.85	11.591 ± 0.90	20.177 ± 0.94

$t_{1/2}$(h)	0.557 ± 0.12	4.388 ± 2.71	6.98 ± 2.85	13.393 ±2.88

[a]Mean ± S.D.; n=6. p< 0.05 PK parameters compared with the pure drug. One-way ANOVA followed by student's t-test.

5.4.3.15*In vivo*anti tumor activity

The results of *in vivo* antitumor activity performed for 30 days after oral administration of the pure drug (CAP), control (saline), standard (doxorubicin), and optimized formulations (F-1, F-2 and F-3) in tumor bearingBalb /c mice is illustrated in Figure 5.37. 415.54 mg/kg was considered a final calculated dose [Food and Administration, 2005].The anticancer activity of the optimized formulations (F-1, F-2 and F-3) were studied for weight loss, tumor volume and mortality parameters. A significant decrease in relative tumor volume (RTV) was observed for all formulations in comparison to control group which was found to be increased. The result of relative tumor volume followed the order of F-3 ≈ F-2 > F-1> pure drug> standard >control group (Figure 5.37 a). Weight loss is reported to be a common problem during cancer treatment. The term cachexia is regarded as the main contributor and termed as loss of lean tissueswith or without loss of fat mass [Balstad et al., 2014].

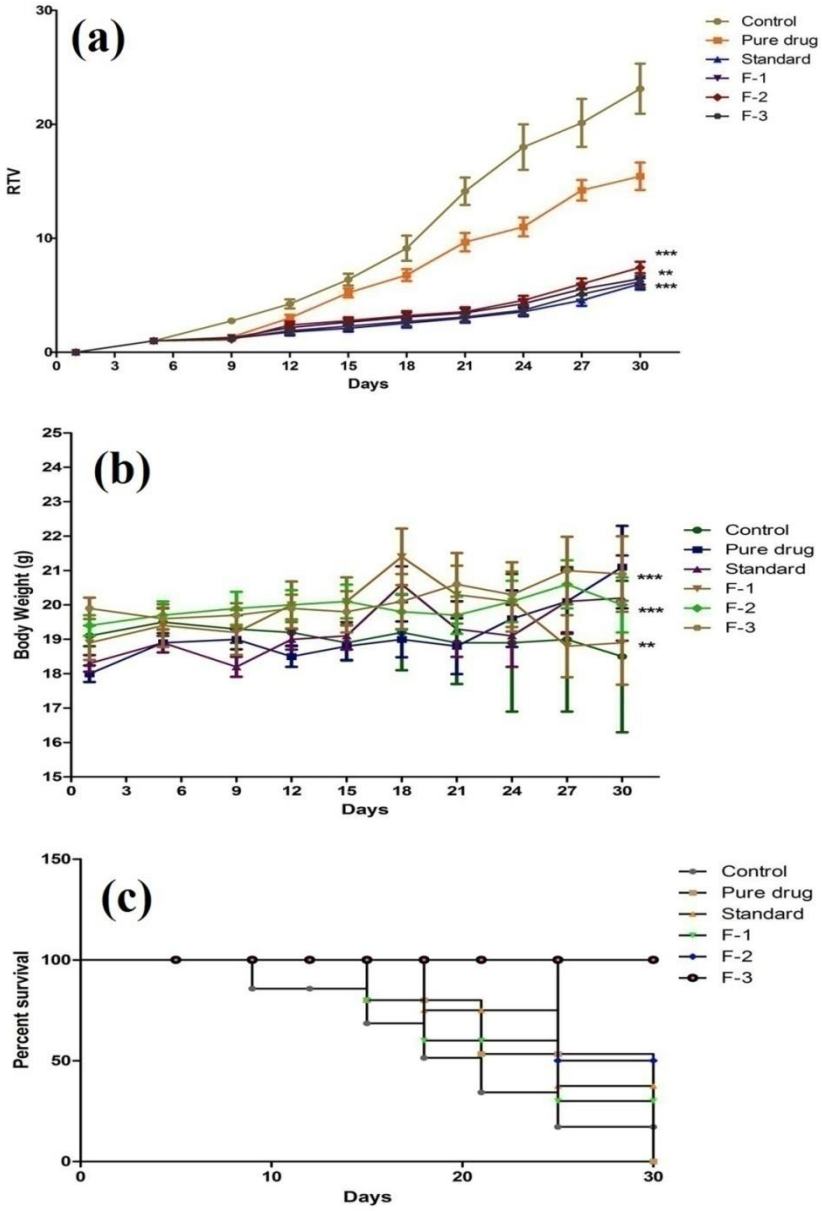

Figure 5.37 *In vivo* antitumor activity in Balb/c mice (a) Relative tumor volume data *versus* number of days in tumor bearing mice in different groups (b) Graph ofaverage weight variation in tumor bearing mice*versus* number of days; (c) Kaplan –Meier non parametric survival curve of differentgroups (vertical bars represent mean ± SEM; n=6; **p< 0.05 and ***p< 0.005.

Thus, to observe the changes in the weight of the animals treated with optimized formulations, standard and pure drug as a function of days was performed (Figure 5.37b). The decrease in body weight was observed in case of control group whereas, the mice treated with standard and optimized formulation showed an increase in their weight and followed the

order F-3≈F-2 > F-1 > Standard >Pure drug> Control. The % survival of animals was expressed by Kaplan- Meier graph (Figure 5.37c) showing 100% survivals of animals in case of optimized formulation (F-3) followed by F-2 83%, F-1 60% standard 67% and pure drug 50% in comparison to control group that showed survival of 17% at the end of 30^{th} day indicating enhanced survival for all five groups (F-1. F-2, F-3, standard and pure drug) in comparison to control indicating safe and effective evidence for treatment of colon cancer.

5.4.3.16 Gamma (γ) scintigraphy study

Gamma scintigraphy study was performed for monitoring the gastroretentivebehaviour of optimized aluminum ion cross-linked buoyant IPN microbeads in mice. Direct radiolabeling method was employed for labelling of microbeads with Technetium -99 (^{99m}Tc).Stannous chloride ($SnCl_2$) was used to reduce ^{99m}TC from higher (heptavalent) oxidation state to lower oxidation state in order to assess the formation of a complex with the formulation (F-3). The entire process was performed at pH 7.4 [Psimadas et al., 2013]. The radiolabeling efficiency of the radiolabeled complex was estimated by instant thin layer chromatography (ITLC) using silica gel as stationary phase and acetone as a mobile phase that was found to be 95.69 ± 0.10% [Patil et al., 2010, Rastogi et al., 2007]. Afterwards, the radiolabeled buoyant IPN microbeads were orally administered to the mice and its images at anterior position were captured by scinti camera (gamma camera), connected with the computer. The images were captured at 0.5 h, 2 h, 4 h and 6 h post administration (Fig.5.38). Due to small size of mice it was difficult to discriminate the organs in GIT, however a marked change in the position of administered radiolabeled microbeads at 0.5 h (5.38 (a)) and 2 h (5.38 (b)) can be observed suggesting the movement of microbeads from mouth to stomach region that remained at the same position till 4 h (5.38 (c)). However, at 6 h the position of microbead was found to be at the lowest position interpreting that it has been moved from its present position i.e. from stomach to downwards i.e. to the intestine region (5.38 (d)). Thus, the prepared

mucoadhesive buoyant IPN microbeads of natural polymers (F-3) is capable of enhancing the gastrointestinal tract residence encapsulating CAP for more than 6 h.

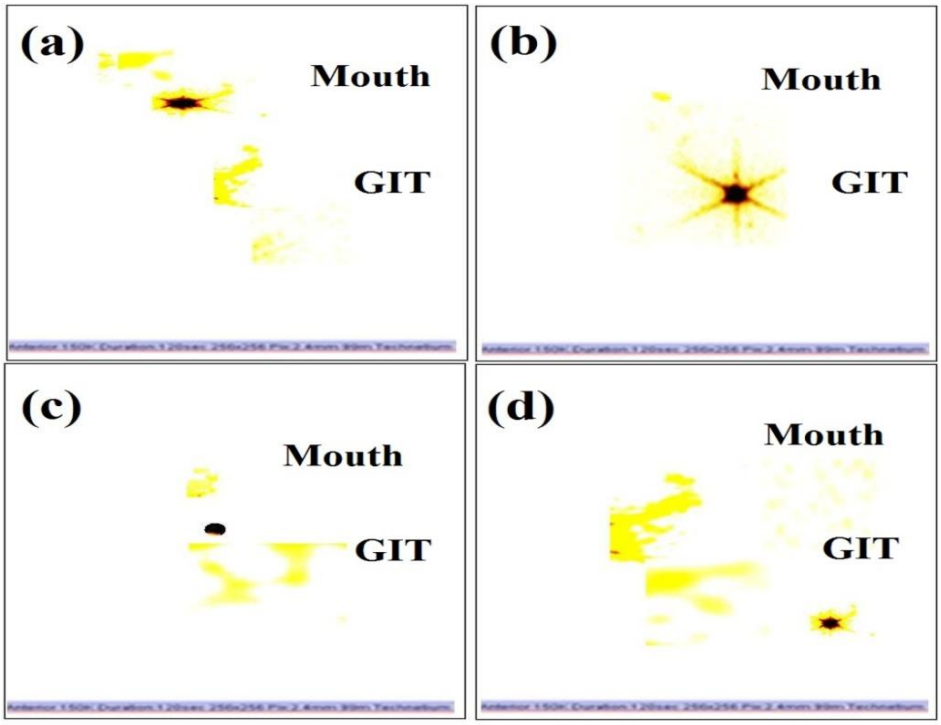

Figure 5.38 γ-Scintigraphic images showing gastro retention of buoyant IPN microbeads at different time interval 0.5 h (a), 2h (b), 4 h (c) and 6 h (d)